

APACIC++ 2.0

A Parton Cascade In C++

F. Krauss*, A. Schälicke§, G. Soff†

Institut für Theoretische Physik, TU Dresden, 01062 Dresden, Germany

August 31, 2018

Abstract

The new version of the parton shower module APACIC++ for the SHERPA event generator framework is presented. It incorporates some features, that are specific for the consistent merging with multi-particle matrix elements at tree-level. This publication also includes some exemplary results and a short description of the upgraded class structure of APACIC++, **version 2.0**.

Key words: QCD, Monte Carlo event generator, parton shower

PACS: 13.87.-a, 13.87.Fh, 13.66.Bc, 13.85.-t

Contents

1	Introduction	2
2	Parton shower	3
3	Implementation	13
4	Results	16
5	Conclusions	30
A	Brief program documentation	31
B	Altarelli–Parisi splitting functions	37
C	Definitions of event shapes	38

*email: krauss@theory.phy.tu-dresden.de

§email: dreas@theory.phy.tu-dresden.de

†deceased

1 Introduction

Event generators for the simulation of high-energetic reactions of particles play an important role in understanding inclusive and exclusive final states at collider experiments. In order to live up to the complicated task of a complete simulation of such processes, event generators decompose the full reaction into a sequence of individual steps, usually divided by a characteristic scale. Typically, the starting point for the simulation of an individual event is the selection of the hardest process in it, commonly this is denoted as the signal process and described at the parton level. The emerging partons are then passed to the parton shower. This part of the simulation describes additional multiple parton emission. In modelling this Bremsstrahlung-like radiation, certain approximations are made, that retain the leading soft or collinear contributions and allow the description of complex radiation patterns through individual parton splittings at decreasing scales. When the splitting scale reaches a cut-off value, typically of the order of a few Λ_{QCD} , the parton shower stops. At these scales, the realm of perturbative QCD is left, and the regime of soft QCD is reached. There, the final translation of the parton to primordial hadrons is modelled through phenomenological approaches. If the primordial hadrons are unstable, they are further decayed until only stable hadrons are left.

In such a framework, the parton shower provides the link between perturbatively calculable differential cross sections at the parton level and models for their transition to observable hadrons with phenomenological parameters, which need to be tuned to data. The inclusion of the parton shower does not only create more realistic high-multiplicity parton final states from low parton multiplicities available through corresponding exact matrix elements, it also reduces the average distance of the partons in momentum space down to a fixed size and thus ensures that the hadronisation parameter tunes are rather independent of the hard process in question. It is this aspect of the parton shower that renders it indispensable for a meaningful simulation with any predictive power. This can then be used in order to calculate hadronisation corrections or to judge detector effects in certain processes. In most cases, results from parton shower Monte Carlos have been in astonishing agreement with data, giving rise to the confidence that simulation tools can also be used to predict signals and backgrounds for the current and the next round of collider experiments.

Although, for more than two decades, parton showers have been widely used in multi-purpose event generators, details of their specific implementation traditionally depend on certain choices and, due to recent developments, on the specific form the hard matrix elements generate the initial parton configurations. Traditional multi-purpose event generators, like `Pythia` [1, 2] or `Herwig` [3, 4] usually have a $2 \rightarrow 2$ process at leading order (LO) as the signal process. There, after defining the corresponding, process-dependent starting conditions for the shower, the latter is allowed to evolve freely. Only recently, this treatment has been consistently extended to next-to leading order (NLO) precision for $2 \rightarrow 2$ processes in the `MC@NLO` framework [5, 6], which uses the machinery of `Herwig`. There, the NLO calculation is modified in order to match the requirements imposed by the specific form of the parton shower. Another approach, going beyond

$2 \rightarrow 2$ processes, has been taken in **SHERPA** [7]; there, a fully automated consistent merging of $2 \rightarrow n$ processes at the tree-level with the parton shower according to the formalism of [8, 9] has been implemented and tested [10]¹. For the merging with such multi-leg tree-level matrix elements, the parton shower has to be supplemented with the determination of more involved starting conditions and with additional constraints on the phase space of the emitted particles.

In this paper the specific realisation and implementation of the parton shower in **SHERPA** will be presented. A first version of this module, **APACIC++**, **version 1.0**, has been published some time ago in [16]; it covered the parton shower in the final state only, including some algorithms for the merging with the matrix elements provided by **AMEGIC++** [17, 18]. In this first version, many of the steering and service classes were still located within **APACIC++**; as time went by, **APACIC++** transformed from a stand-alone code to a mere module of the full framework **SHERPA**. In its present state, **version 2.0**, which is discussed in the following, **APACIC++** thus includes the parton shower in the initial and final state and an improved handling of algorithms necessary for the parton shower aspects of the merging procedure². The outline of this paper is as follows: After briefly reviewing the parton shower formalism in Sec. 2, the ideas underlying its particular implementation in **APACIC++** will be discussed in Sec. 3. There, special focus will be on those aspects, which are specific for the merging procedure with matrix elements. In Sec. 4 exemplary results will be presented, which compare the parton shower results of **APACIC++** with analytical approaches and with data. Details of the implementation, including a short description of the class structure of **APACIC++** will be given in the appendix, App. A.

2 Parton shower

This section comprises a brief overview of the parton shower formalism and the corresponding algorithms implemented in **APACIC++**. There, the sequence of parton emissions in the shower evolution is organised by virtuality as the ordering parameter. In this respect, the algorithm presented here is closely related to the implementation in **Pythia** [1, 2]³. However, the **APACIC++** version differs in some details like the treatment of massive particles and particular scale choices for the evaluation of coupling constants and parton density functions (PDFs). In addition, it incorporates some unique features that facilitate the merging of matrix elements with the parton shower according to the

¹A similar approach for the merging of matrix elements with the dipole cascade [11] has been taken in [12]; for some specific processes the formalism has been used to merge multi-jet matrix elements with **Pythia** and **Herwig** [13]. A slightly different method [14] has been advocated by the authors of **Alpgen** [15], who merge their matrix elements with the parton shower of **Herwig**.

²However, it should be noted that situations like deep-inelastic scattering are still beyond the reach of **APACIC++** and, thus, of **SHERPA**.

³Note that recently, a reformulation of **Pythia**'s parton shower has been presented [19], which employs transverse momentum as ordering parameter. It has been implemented into the recent version of **Pythia** [20]. In [21] an alternative evolution variable, also related to transverse momentum, has been discussed. It has already been implemented into **Herwig++** [22].

formalism of [8, 9].

Basics of parton showering

The parton shower evolution relies on the fact that parton emission processes become singular in the soft or collinear limit. When the available phase space is cut accordingly, these singularities translate into large logarithms, which can be resummed according to the DGLAP evolution [23, 24, 25, 26]. By taking into account the leading logarithms only, the parton shower picture reduces complex radiation patterns of multiple parton emissions to chains of individual independent parton splittings. They are organised in a probabilistic manner by an ordering parameter, usually some quantity like the virtual mass of the decaying parton or the transverse momentum of the decay products. Suitable constraints on this ordering parameter avoid singular regions of phase space. The probability for no parton splitting to occur between two scales $t_0 < t_1$ is encoded in the Sudakov form factor. It is given by

$$\Delta_a(t_0, t_1) = \exp \left\{ - \int_{t_0}^{t_1} \frac{dt}{t} \int dz \frac{\alpha_S(p_\perp)}{2\pi} \sum_{b,c} P_{a \rightarrow bc}(z) \right\}, \quad (1)$$

where p_\perp is the transverse momentum. It can be written as a function of the scale t and the energy splitting variable z . $P_{a \rightarrow bc}(z)$ denotes the splitting function for the branching $a \rightarrow bc$. A complete list of splitting functions implemented in `APACIC++` can be found in App. B. Because of its interpretation as no-splitting probability between two scales, ratios of two Sudakov form factors like

$$P_{\text{nobranch}} = \frac{\Delta(t_0, t_1)}{\Delta(t_0, t)} \quad (2)$$

yield the probability for no emission between t_1 and t , which could be resolved at the scale t_0 . Given a hard starting scale t_1 , this allows the scale for the actual branching t to be generated by equating a random number R with this ratio and solving for t . With a second random number then the splitting variable z can be selected. It is distributed according to

$$P_{\text{split}} = \frac{\alpha_s(p_\perp)}{2\pi} P(z). \quad (3)$$

This probabilistic interpretation allows the formulation of the parton shower as a Markov-chain of independent $1 \rightarrow 2$ -branchings, where the scale t_1 , at which the former splitting occurs, sets the upper limit for the subsequent branching. Organising the parton shower in such a way results in what is known as “forward evolution”. This type of evolution is employed for parton showers in the final state, i.e. for the “time-like parton shower”, where the resulting parton ensemble is not subject of any other constraint.

For the initial state, however, i.e. for space-like parton evolution, the situation changes drastically. This is because standard forward evolution of a parton ensemble from some comparably low fixed hadronic scale $Q_0^2 < 0$, of the order of a few Λ_{QCD} , to the fixed scale

of hard interaction, $Q^2 \ll Q_0^2$, distributed according to the appropriate matrix elements, would be highly inefficient. Therefore it is more convenient to start with specifying the scale Q^2 of the core process and its momentum fractions x_1 and x_2 , and subsequently evolve “backwards” to the partons assumed to be resolved from the incoming hadrons. The correct way to perform this backward evolution has been introduced in [27, 28]; it boils down to modifying the Sudakov form factors by dividing by the appropriate PDF at the given scale and at the relevant Bjorken- x . The resulting no-branching probabilities are then given by⁴

$$P_{\text{nobranch}} = \frac{f(x, t)}{f(x, t_1)} \cdot \frac{\Delta(t_0, t_1)}{\Delta(t_0, t)}. \quad (4)$$

Again, equating this probability with a random number and solving for t defines the previous branching scale. This time, however, the corresponding splitting variable z is distributed according to

$$P_{\text{split}} = \frac{\alpha_s(p_\perp)}{2\pi} \frac{P(z)}{z} f\left(\frac{x}{z}, t\right), \quad (5)$$

where x is the momentum fraction of the decaying parton, and $z = x/x_1$ with x_1 being the momentum fraction of the resulting parton from which the backward step started. In both time-like and space-like evolution, the notion of soft colour coherence [28, 30, 31, 32, 33] plays a crucial role. It results in an angular ordering of subsequent branchings, which can be implemented directly through a corresponding choice of the evolution variable. This has been done in **Herwig** [3, 4], where a suitable angular variable has been chosen. Alternatively, colour coherence can be implemented by choosing transverse momentum as ordering parameter; this choice has been made in **Ariadne** [11] which bases its multiple emission treatment on splitting colour dipoles. Recently, two new formalisms to incorporate ordering according to transverse momentum into the more conventional parton picture have been presented in [19, 21]. In its most trivial version, however, angular ordering can be imposed through a direct veto on increasing opening angles. This is how it has been implemented in **Pythia**, where virtuality is the evolution variable. Of course, such a way of implementing colour coherence is by far not as sophisticated as the methods above; nevertheless this method has also been chosen in the framework of **APACIC++**.

Variables in APACIC++

As indicated above, the parton shower in **APACIC++** is organised in terms of virtuality, i.e. in terms of the virtual mass of the decaying particle, and the splitting variable z is interpreted as the energy fraction of one decay product (daughter) w.r.t. the decaying parton (mother).

⁴A more efficient, non-Markovian, evolution algorithm is currently under investigation [29].

1. Time-like evolution:

For parton branchings $a \rightarrow bc$ in the final state, the evolution variable t is given by

$$t = t_a = p_a^2 = (p_b + p_c)^2. \quad (6)$$

The splitting variable z is defined as energy fraction, i.e.

$$z = \frac{E_b}{E_a}, \quad (7)$$

taken in the rest frame of the complete final state parton shower⁵. For the respective transverse momentum, which serves as an argument in the running coupling constant and as a low-energy cut-off, a definition following [34] has been chosen. There,

$$k_{\perp}^2 = 2 \text{Min}\{E_b^2, E_c^2\}(1 - \cos \theta_{bc}), \quad (8)$$

which in terms of t_a and z translates into

$$k_{\perp}^2 = \text{Min} \left\{ \frac{z}{1-z}, \frac{1-z}{z} \right\} t_a. \quad (9)$$

There is, however, some residual freedom in the exact choice of scales, which can be altered by a (logarithmically) small factor. In **APACIC++**, this freedom is used to **define** the transverse momentum as

$$p_{\perp}^2 = \frac{1}{4} \text{Min} \left\{ \frac{z}{1-z}, \frac{1-z}{z} \right\} t_a. \quad (10)$$

Demanding that all p_{\perp} are larger than some minimal cut-off, $p_{\perp}^{(0)}$, immediately poses a constraint on the allowed (t_a, z) -range for individual branchings, namely

$$t_a > t_0 = 4p_{\perp}^{(0)2} \quad \text{and} \quad z \in \left[\frac{t_0}{t_a + t_0}, \frac{t_a}{t_a + t_0} \right]. \quad (11)$$

In addition, the transverse momentum must be positive. Using the definition of the splitting variable, Eq. (7), yields a kinematical condition on z , namely

$$z \in \left[\frac{1}{2} \left(1 - \sqrt{\frac{t_a}{E_a^2}} \right), \frac{1}{2} \left(1 + \sqrt{\frac{t_a}{E_a^2}} \right) \right]. \quad (12)$$

For the explicit angular veto employed to model coherence effects, the following approximation for the angle is used

$$\theta_{bc} \approx \sqrt{\frac{t_a}{z(1-z)E_a^2}}. \quad (13)$$

⁵In **APACIC++**, the time-like evolution of a given parton ensemble is performed in its rest frame. After the shower terminates, the resulting partonic final state is fully reconstructed and boosted into the relevant (lab) frame.

It stems from $t_a = 2z(1-z)E_a^2(1 - \cos\theta_{bc})$. This approximation is valid for small θ_{bc} , but it can conveniently be used for large angle emission too, since the actual value is irrelevant for its role as ordering parameter.

Having split parton a into b and c , the two offsprings are massless first. They gain a virtual mass by continuing the parton shower evolution for another step with starting scale t_a . Of course, the sum of their virtual masses cannot be larger than the virtual mass of a , i.e.

$$\sqrt{t_b} + \sqrt{t_c} < \sqrt{t_a}. \quad (14)$$

This, together with the angular ordering constraint, sets some additional limits on the splitting variables. However, there is still an issue to be resolved: When z was defined, it was implicitly assumed that both outgoing partons are on their mass-shell; this is not true any longer, which implies that the branching kinematics of $a \rightarrow bc$ has to be redefined. In `APACIC++`, this is achieved through a redefinition of the energy splitting variable z , also quite along the lines of what happens inside `Pythia`. In both codes, the modified splitting variable reads

$$\tilde{z} = \left(z - \frac{1}{2}\right) \frac{\lambda(t_a, t_b, t_c)}{t_a} + \frac{t_a + t_b - t_c}{2t_a}, \quad (15)$$

where

$$\lambda(a, b, c) = \sqrt{(a - b - c)^2 - 4bc}. \quad (16)$$

This modification constitutes a simple linear transformation from the massless to the massive domain, which is always possible as long as the condition given by Eq. (14) is satisfied.

If one or more of the partons a , b , and c are massive, the definitions above change as follows:

- The evolution variable is now defined as $\tilde{t}_a = t_a - m_a^2$. This in addition to the usage of mass terms in the splitting kernels (cf. App. B), leads to a slightly modified Sudakov form factor.
- The argument of the running coupling is now given by the “complete” k_\perp formula, i.e. it is defined through

$$p_\perp^2 = \frac{\text{Min}\{E_b^2, E_c^2\}}{2}(1 - \cos\theta_{bc}), \quad (17)$$

which assumes on-shell, but not necessarily massless daughters.

The other conditions introduced above are, in principle, not altered, provided that the kinematical variable t_a is used rather than the evolution variable \tilde{t}_a . Consequently, the kinematical z -domain is still given by Eq. (12), and z is translated into the massive case by Eq. (15). This leads to a reinterpretation of the splitting variable, which is necessary, since the splitting functions are calculated with z being the light-cone momentum fraction.

2. Space-like evolution:

For the parton shower in the initial state, i.e. space-like showers, the evolution proceeds backwards. The ordering parameter here is the virtual mass of the respective initial state parton. Therefore in branchings $b \rightarrow ac$ the scale is given by

$$t = t_a = p_a^2 < 0, \quad (18)$$

and, wherever it is needed, the absolute value is taken. The definition of the splitting variable is a little bit more tricky. In order to ensure four-momentum conservation in the reconstruction of the showering kinematics, the two shower branches of the two incoming partons are coupled. For the two incoming particles, labelled by a and \tilde{a} , the Sudakov form factors, cf. Eq. (4), are used to choose their virtual mass, t_a and $t_{\tilde{a}}$. The parton with larger off-shellness is selected for the reconstruction of the corresponding backward step. Assume that $t_a < t_{\tilde{a}}$, and, hence, that a is selected. Then z is defined through

$$z = \frac{(p_a + p_{\tilde{a}})^2}{(p_b + p_{\tilde{a}})^2}, \quad (19)$$

clearly a Lorentz-invariant measure. This implies that, step by step, the c.m. energy squared in the parton system is enhanced by a factor $1/z$. In the same way, the Bjorken- x of partons a and b are related by

$$x_b = x_a/z, \quad (20)$$

where the first Bjorken- x of the partons entering the hard process are taken directly from the matrix element evaluation. In this respect, at each step of the space-like shower evolution, the current pair of partons is oriented along the beam axis, with Bjorken- x as if they were massless. It is this Bjorken- x and a scale $Q^2 = p_{\perp}^2$ that constitute the parameters for the calculation of the PDF at the corresponding step. In the c.m. system of partons b and \tilde{a} , the transverse momentum of a and c is given by

$$k_{\perp}^2 = -(1-z)t_a. \quad (21)$$

Following a similar reasoning as in the final state treatment, the transverse momentum entering the running coupling as well as the PDF evaluation is **defined** through

$$p_{\perp}^2 = -\frac{1-z}{4}t_a. \quad (22)$$

Having thus constructed the backward step $b \rightarrow ac$ leading to the parton b , it is clear that c may experience a final state shower evolution. Its starting scale, by default, is given by t_a . For kinematic reasons, however, the actual scale that is chosen in the shower evolution must also satisfy

$$t_c < t_{c,\max} = \frac{\lambda_{a\tilde{a}}\lambda_{b\tilde{a}} - s_{a\tilde{a}}s_{b\tilde{a}}}{2t_{\tilde{a}}} + t_a + t_{\tilde{a}} \quad (23)$$

with

$$s'_{a\bar{a}} = s_{a\bar{a}} - t_a - t_{\bar{a}}, \quad s'_{b\bar{a}} = s_{b\bar{a}} - t_b - t_{\bar{a}} \quad (24)$$

$$\lambda_{a\bar{a}} = \lambda(s'_{a\bar{a}}, t_a, t_{\bar{a}}) \quad \lambda_{b\bar{a}} = \lambda(s'_{b\bar{a}}, t_b, t_{\bar{a}}) \quad (25)$$

where $s_{a\bar{a}} = (p_a + p_{\bar{a}})^2$ and $s_{b\bar{a}} = (p_b + p_{\bar{a}})^2 = s_{a\bar{a}}/z$. Similar to the approximation of Eq. (13), the opening angle of this splitting can be estimated by

$$\theta_{ac} \approx \sqrt{\frac{t_a}{(1-z)E_a^2}}. \quad (26)$$

Knowing t_b and t_c as well as the four-momenta p_a and $p_{\bar{a}}$, the four-momenta p_b and p_c are constructed explicitly in the c.m. frame of p_a and $p_{\bar{a}}$. In this system, energies and momenta are fixed according to

$$E_c = \frac{s_{b\bar{a}} + t_b + t_a - t_c}{2\sqrt{s_{a\bar{a}}}} \quad (27)$$

$$p_{z,c} = \frac{s_{b\bar{a}} - 2E_{\bar{a}}E_c}{2p_{z,a}} \quad (28)$$

$$p_{\perp c} = \sqrt{E_c^2 - p_{z,c}^2 - t_c}, \quad (29)$$

where the transverse momentum is distributed uniformly in its azimuthal angle. Furthermore,

$$p_b = p_a + p_c. \quad (30)$$

Subsequently, the system is boosted into the rest frame of partons b and \bar{a} and rotated such that their momenta point along the beam axis.

Colour treatment

When the parton shower terminates, the resulting multi-parton ensemble needs to be transformed into hadrons. Due to a lack of quantitative understanding of non-perturbative physics, this is achieved through phenomenological models. These models have some different underlying physics assumptions, highlighted by the examples of the string model [35, 36, 37, 38, 39, 40] stressing the role of colour coherence [41], and of cluster fragmentation models [42, 43, 44, 45, 22] that are closer to the independent fragmentation approach [46] and the concept of pre-confinement [47]. However, they have in common that they rely on having as input a parton ensemble with a well-defined colour structure in the $N_c \rightarrow \infty$ limit. This necessitates that the parton shower must distribute colours in this limit. In most cases, like, e.g. in a splitting $q \rightarrow qg$ the colour structure is unambiguously defined, ensuring that a well-defined colour structure at the beginning of the parton shower evolution can be mapped onto a well-defined colour structure at its end. However, there are cases with ambiguities, namely in splittings of the type $g \rightarrow gg$.

In this case, there are two ways of locally distributing colour. Denoting a colour state by its colour triplet and anti-triplet labels in the $N_c \rightarrow \infty$ limit, (a, \bar{b}) , these two ways in the splitting $g(1) \rightarrow g(2)g(3)$ can be visualised as

$$(a, \bar{b}) \rightarrow (a, \bar{c}) + (c, \bar{b}) \quad \text{or} \quad (a, \bar{b}) \rightarrow (c, \bar{b}) + (a, \bar{c}). \quad (31)$$

In APACIC++, the choice is made in the following way: In the shower evolution, the decaying gluon 1 was produced in another parton branching process, where the other decay product is colour-connected to the gluon. For both gluons 2 and 3, the transverse momentum w.r.t. this colour partner is determined according to Eq. (9). The choice is then made such that the gluon with the smaller relative k_\perp is colour connected with this partner parton.

Initialisation of the parton shower

Within the SHERPA framework, an algorithm along the lines of [8, 9] for the consistent merging of tree-level matrix elements for multi-particle production with the parton shower of APACIC++ has been implemented [48]. The key idea of this algorithm is to separate the phase space for parton emission into the hard region of jet production accounted for by suitable tree-level matrix elements and the softer region of jet evolution covered by the parton shower. Then, extra weights are applied on the former and vetoes on the latter, such that the overall dependence on the separation cut is minimal. The separation is achieved through a k_\perp measure [34, 49, 50]. The weight attached to the matrix elements is constructed employing Sudakov form factors, thereby taking into account those terms that would appear in a corresponding parton shower evolution. Therefore, a “pseudo parton shower history” is reconstructed by clustering the initial and final state particles from the tree-level matrix element according to the k_\perp algorithm. This procedure provides the scales necessary for the evaluation of the weight, namely the nodal values of the different k_\perp , where two jets have been merged into one. Within APACIC++, the reconstructed “shower history” is utilised for the determination of initial conditions for the shower evolution. Then, starting from the hard $2 \rightarrow 2$ core process, all partons obtain as starting scale for their shower evolution the nodal virtuality, where they emerge for the first time. It should be stressed at this point that there is some residual mismatch in the parton shower variables used in APACIC++, namely virtuality $t = p^2$, and the scales (k_\perp measures) used in the Sudakov form factors employed in the reweighting of the matrix elements. This point will be discussed in more detail in the following section.

For the scale of the four partons entering or leaving the $2 \rightarrow 2$ process, there are a few options, defining the respective choice of scale t_{start} :

- Processes of the type $e^+e^- \rightarrow q\bar{q}$: $t_{\text{start}} = \hat{s} = (p_q + p_{\bar{q}})^2$.
- Drell-Yan type (e.g. $q\bar{q} \rightarrow e^+e^-$): $t_{\text{start}} = \hat{s} = (p_q + p_{\bar{q}})^2$.
- “Drell-Yan+jet”-type (e.g. $q\bar{q} \rightarrow W^{(*)}g$): For the incoming partons the choice is $t_{\text{start}} = \hat{s} = (p_q + p_{\bar{q}})^2$. For the final state parton, however, the start scale for the

shower evolution is different, namely the nodal value where it has been produced, usually \hat{t} or \hat{u} .

- QCD processes: In this case, different colour flows are usually competing. The winner is selected according to the respective contribution, which is related to a specific propagator structure (\hat{s} -, \hat{t} -, or \hat{u} -channel). The choice of starting scale follows the selection of the colour structure; in most cases therefore the starting scale t_{start} is the minimum of \hat{t} and \hat{u} .

In order to account for colour coherence, a maximal allowed branching angle θ_{crit} has to be determined for each parton. Using the knowledge of the colour connections of the $2 \rightarrow 2$ process, θ_{crit} is defined as the angle between the parton in question and the parton colour connected to it. In case of gluons the choice of this angle is, of course, ambiguous; there, the maximum of both possible values is taken.

Having fixed the starting scales of the hardest partons, the starting scales for the evolution of softer partons are easy to obtain. In principle, there are only two ways, in which softer partons may emerge, which lead to a slightly different treatment.

- Branchings in the final state:
There the harder, i.e. the more energetic, of the two offsprings inherits as starting scale and angle the values of the decaying parton, whereas the parameters of the softer offspring are taken directly from the node. In other words, the initial virtual mass equals the invariant mass of the pair, and the starting angle is given by its opening angle.
- Branchings in the initial state:
There, in analogy to the treatment of the space-like shower evolution, the virtual mass and the starting angle of the time-like offspring are given by the virtual mass of the initial state parton that branches “backwards” and the respective opening angle w.r.t. the corresponding beam. The “new” initial state parton inherits the starting scale and angle of the line pointing towards the “core” process.

Merging issues

Having fixed the starting scales, the parton shower can be evolved. Due to the merging prescription, emissions inside the parton shower have to be vetoed, if they result in the production of partons with transverse momenta k_{\perp} larger than a given jet resolution scale, p_{\perp}^{cut} . Parton showers attached to matrix elements with the highest multiplicity must live up for the production of eventual extra jets. In this case, the veto scale is not the jet resolution scale but rather given by the smallest k_{\perp} of the partons stemming from the matrix element.

However, in the parton evolution of such multi-parton final states, there is a last subtlety. It is connected to the fact that, through showering, the partons may acquire a virtual mass different from their on-shell mass used in the matrix element. This recoil has to be compensated for, if possible in such a way that the other partons stemming from the

matrix element are least perturbed. This is solved in the following way: The merging procedure results in the reconstruction of a pseudo parton shower history of the parton ensemble. Thus, to each parton produced in the matrix element a partner can be assigned such that both emerge in a branching of the pseudo parton shower history. If one of them or both acquire a mass, the respective partner takes care of the recoil. The strategy employed for this is very similar to the one used when the initially massless partons in the showering acquire a mass; in both cases the energy splitting variable is shifted through a linear transformation, for the shower case, cf. Eq. (15). In the initial branchings of the shower initiators, there are two cases to be considered:

- Both partners experience a parton shower evolution. Then, the reconstructed energy splitting variable of the branching where they have been produced, is shifted according to Eq. (15).
- In the branch $a \rightarrow bc$, only one partner (b) experiences a parton shower evolution, the mass of its partner is (c) fixed, since it can be thought of as an internal line of the matrix element - it branches according to the pseudo parton shower history. Then z is shifted according to

$$\tilde{z} = \left(z - \frac{t_a + t_b^{(0)} - t_c^{(0)}}{2t_a} \right) \frac{\lambda(t_a, t_b, t_c)}{\lambda(t_a, t_b^{(0)}, t_c^{(0)})} + \frac{t_a + t_b - t_c}{2t_a}, \quad (32)$$

where $t_i^{(0)}$ denote the matrix element masses and t_i the new virtualities. This modification results in a change of the opening angle θ_{bc} , leading to a modified momentum even for the particle with the mass unchanged. In order to comply with four-momentum conservation, its offsprings have to be adjusted, too. This transformation can easily be achieved through a rotation followed by a boost along the direction of particle c .

Within APACIC++, an additional veto on “losing” a jet produced in the matrix element is introduced. Losing a jet through the shower is possible due to a mismatch of the quantities responsible for jet definition (k_{\perp}) and jet evolution (virtual mass). This leads to recoils imposed by the shower evolution resulting in a change of k_{\perp} , while the virtuality of the internal line in question is preserved. Therefore, a check on the number of jets is performed after the shower evolution is finished. This is done by demanding that the - now off-shell - shower seeds are still separated in k_{\perp} . If this is not the case the event is rejected, and a new event is generated from the beginning, i.e. with a new kinematical situation but the same flavour constellation of the jets.

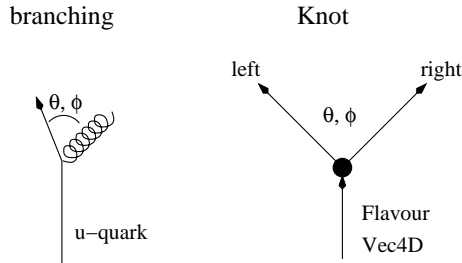


Figure 1: The basic building blocks of shower emission are binary branchings, represented by `Knots`.

3 Implementation

This section focuses on the basic strategies according to which the formalism discussed in the previous section, Sec. 2, is implemented in `APACIC++`. A more detailed reference to all individual classes can be found in App. A.

The basic unit for the realisation of the parton shower in terms of a computer program is the individual branching of a single parton. Connecting such branchings automatically leads to the Markov structure of the full emission pattern. In other words, the task of a parton shower program is to fill and to connect such individual branchings. It is the strength of an object-oriented programming language like `C++` that it is well suited to map the underlying physical pictures onto program code by using an appropriate class structure.

Representation of the parton shower

Following the reasoning above, the basic structure representing a single branching is a `Knot`, reflecting the $a \rightarrow bc$ binary decay structure inherent to the parton shower. A `Knot` carries information on the incoming particle a , encoded in the class `Particle`, and on the `Knot`, where it originates from. When it is filled, i.e. when the decay is specified, it also yields the two offsprings and their respective decay `Knots`. In addition, a number of other quantities are stored in a `Knot`, namely

- the scale t_a ,
- the energy splitting parameter z ,
- the squared energy, E_a^2 ,
- and its minimal virtuality $t_a^{(0)}$,
- the respective opening angle in the approximation of Eqs. (13, 26) θ_{bc} ,
- the azimuthal angle ϕ ,
- and the Bjorken- x of the particle x_a (if needed).

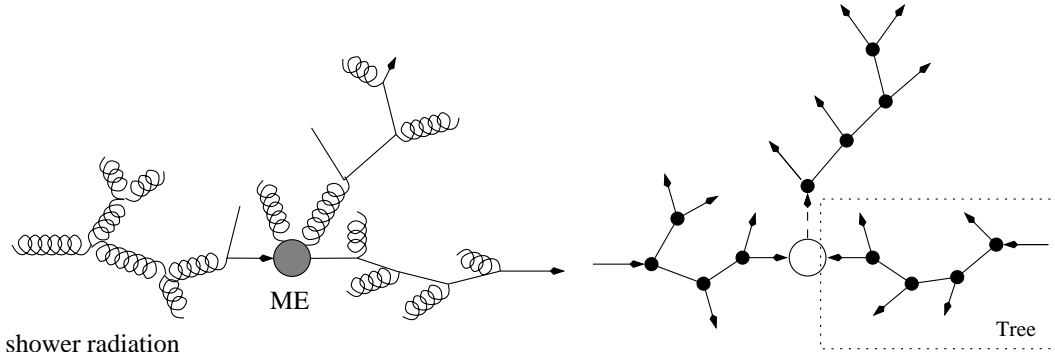


Figure 2: Sketch of the mapping between radiation processes and the corresponding classes. The full radiation pattern is identified as a chain of $1 \rightarrow 2$ processes, a Markov chain, which translates into the class `Tree`. A `Tree` in turn is realised as a list of linked `Knots`. The shower evolution of an event is represented by three `Trees`, one for the final state shower, and two for the initial state shower.

These `Knots` are then linked in terms of a (binary) Markov chain, represented in the class `Tree`. Each `Tree` contains a pointer to its first `Knot`, the root `Knot`⁶. Starting from this root `Knot`, all other `Knots` are then accessible by successively following the pointer inside the `Knots`, thereby spanning the full `Tree` structure. Each event consist of three `Trees`, as indicated in Fig. 2; one `Tree` gives rise to the complete final state shower, eventually with a dummy particle as root `Knot`. The other two `Trees` represent the initial state showers from both sides, therefore they have one of the two particles entering the hardest subprocess as their respective root `Knot`. Since the full parton shower evolution is represented by these `Trees`, they provide routines to create and delete individual `Knots`, or to boost and rotate the full structure. The latter option is relevant for the transparent implementation of the initial state parton shower.

Filling the Trees

The `Trees` are now to be filled by the corresponding parton shower. In `APACIC++`, two classes are responsible for this, namely the `Final_State_Shower` and the `Initial_State_Shower`, who have access to one or two `Trees`, respectively. Since the latter, the `Initial_State_Shower`, produces particles that may undergo a time-like shower evolution, it also has a pointer to the former, the `Final_State_Shower`. Apart from switches steering the specific way the shower works⁷, however, both showers need information from Sudakov form factors and they have to construct the respective time-like or space-like kinematics. These necessities are encoded in corresponding classes, named `Timelike_Sudakov` or `Spacelike_Sudakov`, and `Timelike_Kinematics` or `Spacelike_`

⁶Since a parton shower history is reconstructed in the merging procedure, this root `Knot` may reflect the already fully defined splitting of an internal line of some matrix element.

⁷There are some options for specific questions made available in `APACIC++`, that go beyond the standard settings discussed above.

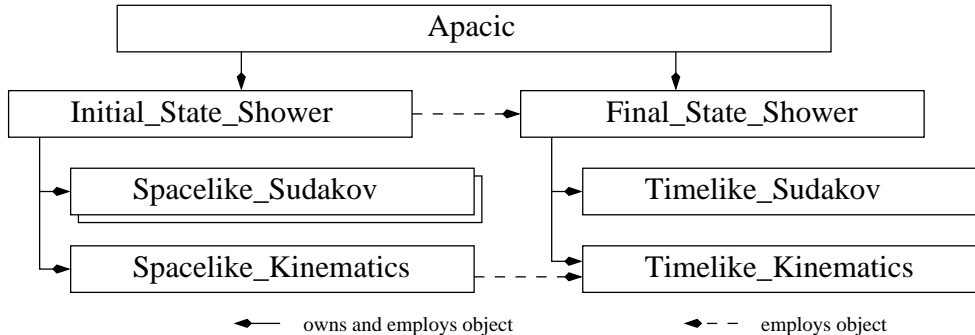


Figure 3: Relation of the main classes of APACIC++.

Kinematics. It is clear that the **Spacelike_Kinematics** must use methods from its time-like counterpart, hence it has a pointer to **Timelike_Kinematics**. Since the two **Kinematics**-classes are responsible for jet vetoes, they have a pointer to a **Jet_Finder** class made available through the **SHERPA** framework and some flags steering its proper usage. An overview over the basic relations between the main classes of APACIC++ is depicted in Fig. 3.

In contrast to the **Kinematics** classes, the two **Sudakov** classes are a bit more intricate. Since most of their actions are related to the selection of splitting functions and their usage, both are derived from the class **Splitting_Group**, and contain a **Splitting_Group** for each flavour, the shower can handle. Then, each **Splitting_Group** builds a wrapper around all splitting functions $P_{a \rightarrow bc}(z)$ for all branchings allowed for a certain incoming particle a . As an example, consider the case of a gluon. It may undergo either a $g \rightarrow gg$ or a $g \rightarrow q\bar{q}$ branching, each of which is represented by its corresponding **Splitting_Function**. Consequently, the class **Splitting_Group** responsible for the gluon branching contains one **Splitting_Function** for the gluon final state and one for each quark flavour. Any individual **Splitting_Function** incorporates information like its incoming and outgoing flavours, an estimate for its integral over z , and methods to extract z distributed according to $P_{a \rightarrow bc}(z)$. In addition, **Splitting_Groups** allow to select a splitting mode and the corresponding flavours.

The two **Sudakov** classes construct all such **Splitting_Groups** for physical branchings. When a parton, encoded in **Knot** is to be split, the respective Sudakov form factor implementation selects the physically relevant **Splitting_Group**, i.e. the one with the flavour of the parton as incoming or outgoing particle, and uses its estimated z integral to select a corresponding t ⁸. Then vetos are applied, either in the procedure of the hit-or-miss method used in the **Sudakov** classes, or in the framework of the merging procedure to reject unwanted jets to be produced in the parton shower. The latter test is performed with the help of the corresponding **Kinematics** class. It should be noted that the **Spacelike_Sudakov** classes contain a PDF due to the backward evolution described above; in view of the possibility to have two different beam particles with

⁸Other information needed for this selection, like the start scale t_{start} and the maximally allowed angle θ_{crit} are obtained from the **Knot**.

different PDFs the class `Initial_State_Shower` has two of them.

4 Results

In this section some results will be presented that validate the implementation of the parton shower algorithms, discussed in the previous sections.

Comparison with analytic Sudakov form factors

First of all, the parton shower of `APACIC++` will be confronted with known analytical results dealing with the resummation of large logarithms emerging in multiple parton emission. Such results are available mainly for e^+e^- annihilation into hadrons. There, analytical calculations describe the relative rates for different jet multiplicities in the k_\perp algorithm. For the massless case, results can be found in [34], massive quarks are dealt with in [51]. All results presented here relate to e^+e^- annihilations at $E_{\text{c.m.}} = 91.2$ GeV, i.e. to the LEP 1 energy.

To gain some first idea about the behaviour of the merged cross sections and the effect of the Sudakov form factors, consider Fig. 4. There, tree-level cross sections for the production of up to four jets, out of which two may be b -jets (left) are contrasted with the weight applied to them in the merging procedure (right). The jets are defined through a Durham jet measure with resolution parameter y , which represents the minimal relative transverse momentum of two separated jets. Already here, it becomes apparent that the massive b -quarks are suppressed w.r.t. massless ones in the cross section, whereas the weights are nearly identical for massless and massive jets. In Fig. 5 the merging has been performed; in the left plot the resulting jet cross sections and their sum are shown for the massless case, the right plot exhibits the corresponding cross sections when two b quarks are involved. It is surprising how stable the total cross sections are w.r.t. the jet definition cut. In Fig. 6 the resulting two- and three-jet rates are displayed. Clearly, due to the “dead cone” effect the b -quarks tend to radiate less, leading to an enhanced two jet rate compared to light quarks. For three jets, the situation is slightly different; for small value of y it is the four-jet rate that starts dominating. In this region therefore the three-jet rate for massive quarks starts to exceed the massless one, which tends to have a larger fraction of four-jet events.

In Fig. 7, the results of the parton shower as implemented in `APACIC++` are confronted with these analytical jetrates, which basically represent a resummed tree-level calculation. The agreement over a wide range of phase space, down to small values of $y \leq 0.004$ is very good. Only for very small values of y the three-jet rate as obtained from the parton shower starts to overshoot the analytical result, which is due to the increased importance of four-jet events in this region. Finally, Fig. 8, exhibits the ratio of three-jet rates with b -quarks and with light quarks (u , d , and s) only. There, data from the Delphi collaboration [52] are contrasted with a full next-to leading order calculation [53] with varying b quark mass, with the pure parton shower result as obtained by `APACIC++` and with the result of the combined matrix element plus Sudakov weight. The data

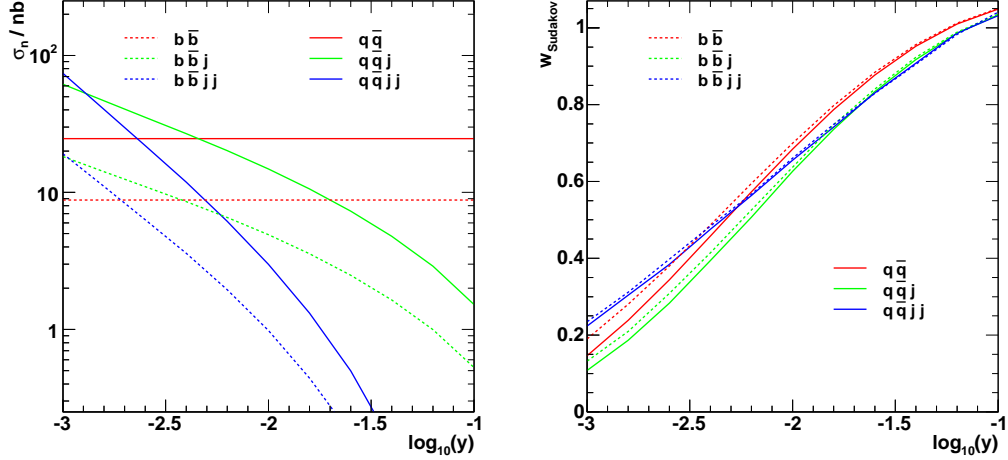


Figure 4: Cross section for the production of up to four jets (left) and the corresponding Sudakov weight that will be attached in the merging procedure (right) vs. the jet resolution y . Two/three/four jet topologies are depicted in red/green/blue, massless jet-configurations are shown with solid lines, jet configurations involving two massive b quarks with $m_b = 4.5$ GeV are shown with dashed lines.

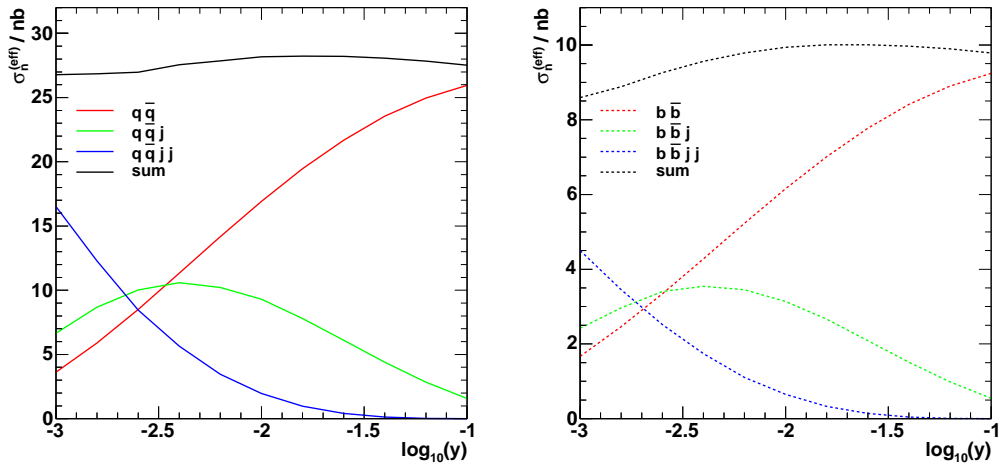


Figure 5: Cross section times Sudakov weight vs. the jet resolution y for each jet configuration and the sum of them. The left plot shows massless jets, the right one displays jet configurations with two massive b quarks.

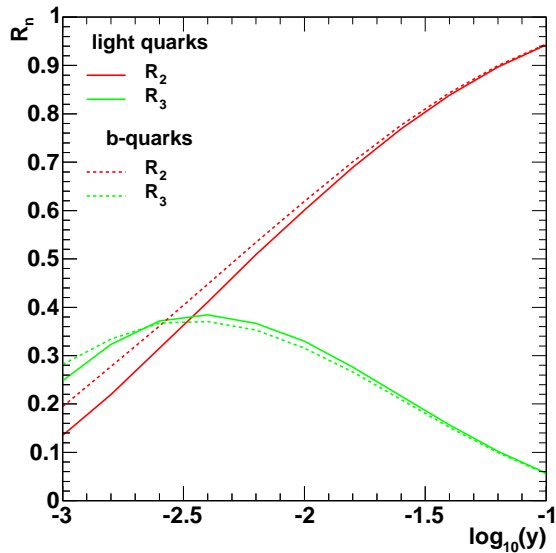


Figure 6: Jetrates for two- and three jets from the combined matrix element plus Sudakov weight.

clearly prefer a lighter b quark with $m_b \approx 3$ GeV in the NLO calculation⁹. In addition, the parton shower obviously describes the data surprisingly well; for the merged matrix element plus Sudakov weight result, a running b quark mass seems to be also appropriate.

⁹This result is consistent with the value obtained by evolving the measurement at the Υ resonance up to the Z boson mass, cf. [52].

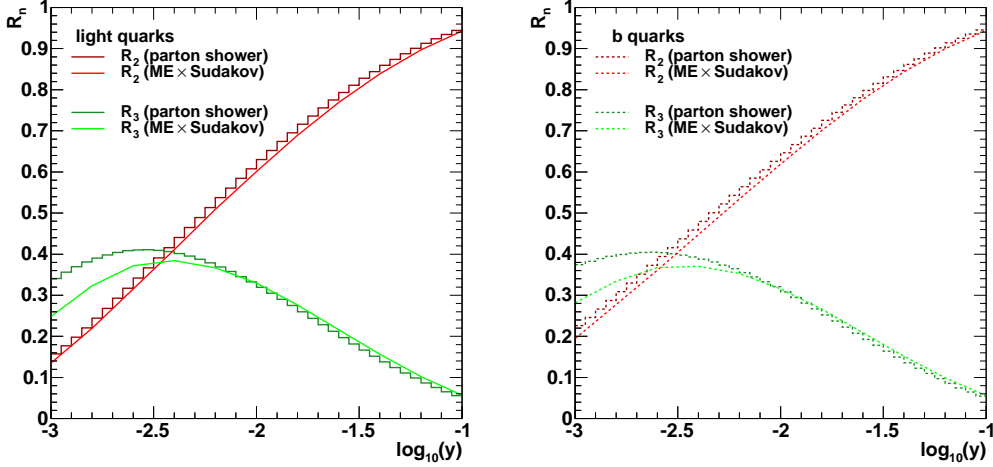


Figure 7: Analytical results for the jetrates from Fig. 6 vs. the results obtained from the parton shower.

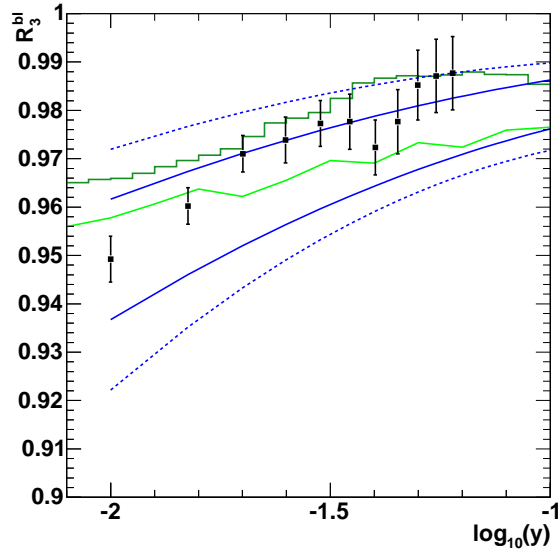


Figure 8: Heavy-to-light three-jet rate ratio $R_3^{bl} = R_3^{(b)}/R_3^{(uds)}$ in dependence on the Durham jet resolution y . Data (black points) from a Delphi measurement [52] are shown together with the SHERPA prediction (the dark green histogram corresponds to the shower result and the light green curve is obtained by combining matrix elements with Sudakov weights), and with an analytic calculation [53] (blue lines, dashed=LO, solid=NLO) for two different values of m_b , $m_b = 3, 5$ GeV.

Comparison of shower and hadron level: Hadronisation corrections

Before further comparing results of the parton shower with experimental data, it must be stressed that many of such comparisons are feasible and meaningful on the hadron level only. This implies that the partons emerging from the shower must be hadronised with some phenomenological model. In the case of **SHERPA**, the choice at the moment is to employ the Lund string model for it. This model has a number of parameters to be tuned to data. The tuning of Monte Carlo event generators to data is an intricate procedure, involving an optimisation in a multi-dimensional phase space of parameters. These parameters may be perturbative (like, for instance, α_s), or non-perturbative (like, for example, the string tension in the Lund model), or they could characterise the transition between the perturbative and the non-perturbative regime (e.g. the parton shower cut-off). For further details on such a tuning procedure, the reader is referred to [54, 55]. The parton shower of **APACIC++** in its versions 1.0 and 2.0 together with the Lund string model implemented in **Pythia** has been tuned in [56] and [57], respectively.

Hadronisation and the tuning of phenomenological models, however, induces some source of systematic error in any simulation that needs to be investigated. In Fig. 9 the parton shower results for total jet rates in the Durham scheme for 2-5 jets are confronted with results after hadronisation. Evidently, both results coincide on a level of 10% or better down to jet resolutions of $y \approx 0.001$. This corresponds to relative transverse momenta of the order of 3 GeV, a kinematical regime, where decays of b -hadrons start to matter. This also implies that down to such low values parton shower results can be compared directly to data. In Fig. 10, two event shape variables, thrust and oblateness, are studied. Again, results before and after hadronisation are compared. Pictorially speaking, thrust is a measure for how “jetty” an event is. A thrust of 1, for example, describes a perfect, “pencil-like” two-jet event, where both jets are oriented back-to-back and have no transverse spread. Clearly, such a configuration is severely suppressed at the hadron level, since it corresponds to events with few, highly collinear particles only. Thus, in the $T = 1$ bin, hadronisation corrections are large. Over a wide range of thrust values away from such extreme configuration, however, the shapes of the results before and after hadronisation are nearly identical; hadronisation corrections in this region therefore are just a constant that can be taken directly from data. In this region of, say, $0.05 \leq T \leq 0.6$, the parton shower results can be confronted directly with data. Similar reasoning holds true not only for the other exemplary observable, oblateness, but for a plethora of observables.

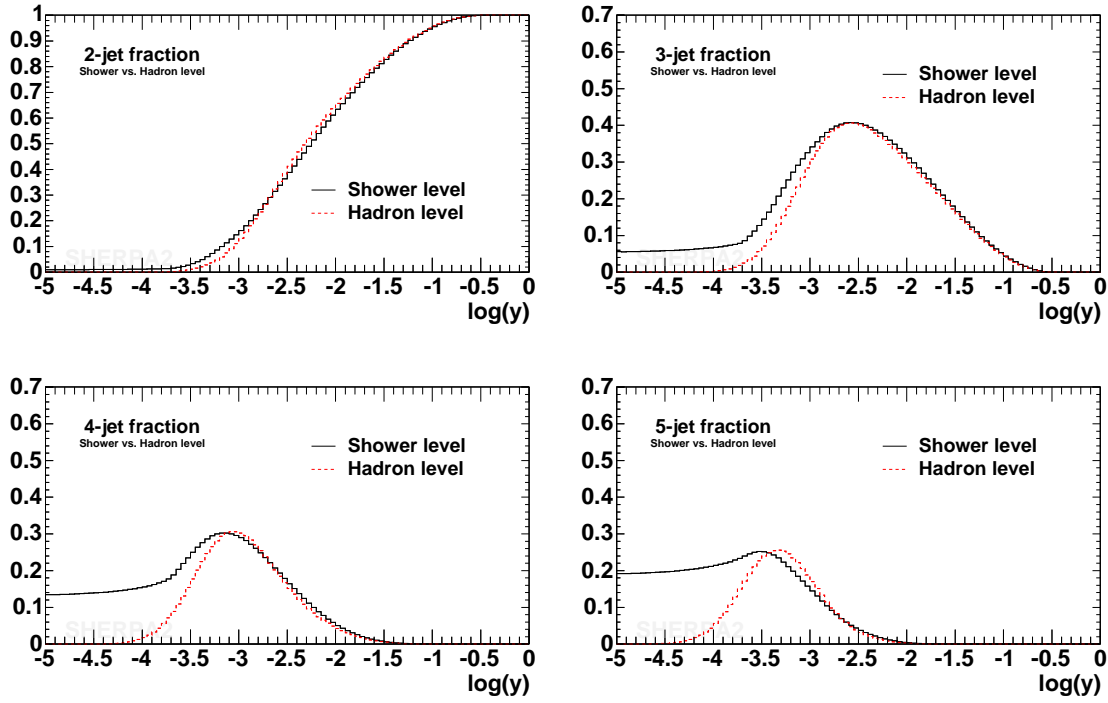


Figure 9: Durham jet rates at LEP 1. The shower level result (solid lines) of SHERPA is contrasted with its result after hadronisation (dashed lines).

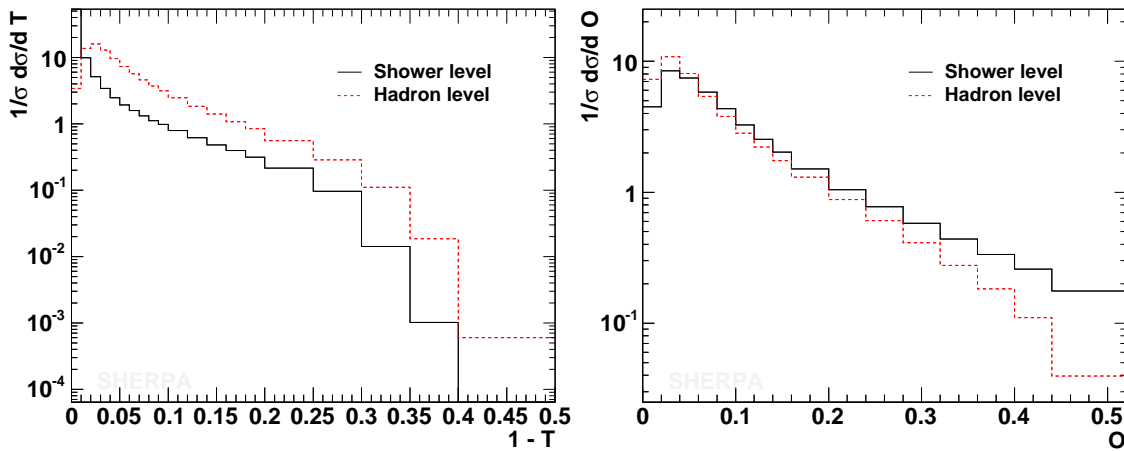


Figure 10: Thrust and Oblateness at LEP 1. The shower level result (solid lines) of SHERPA is contrasted with its result after hadronisation (dashed lines).

Comparison with experimental data from LEP

Having validated the numerical correctness of the parton shower implementation, the focus shifts from the investigation of the behaviour of the Sudakov form factors to the study of experimental observables. There, experimental data can be confronted with the results obtained with the parton shower, eventually after a merging with multijet matrix elements. As mentioned above, in the previous section, the considered data are on the hadron level, consequently a hadronisation model has to be applied. The parameters of the model were tuned, the perturbative input consisted of a sample of multijet matrix elements for up to five jets, merged with the parton shower of **APACIC++**. The quality of the tuning can be judged by considering the multiplicity distribution of charged hadrons and of their scaled momentum, cf. Fig. 11. In this plot as well as in each of the following ones, data are confronted with the parton shower implemented in **APACIC++** (solid lines) and with the merged multijet matrix element plus parton shower (dashed lines), both after hadronisation. For the merged results, contributions from different jet multiplicities are indicated in different colours. Clearly, the merged sample tends to produce a slightly larger fraction of events with harder jets, leading to higher parton and hadron multiplicities; this is visible from the fact that the “parton shower only” sample slightly undershoots the bins with comparably high hadron multiplicity. For the momentum distribution, however, this minor trend washes out. In both cases, the results obtained from the simulation show excellent agreement with data, this is even more so when taking into account that in all plots shown the statistical errors on the Monte Carlo results are of the same order as the experimental errors, indicated by the yellow error bands. The first real test of the parton shower performance is to check whether it is able to reproduce event shape observables, such as thrust, major, the C-parameter, or oblateness¹⁰, cf. Figs. 12 and 13. In all cases, the agreement of the data with the generated events is excellent. In the “parton shower only” sample the trend mentioned above, namely of being a little bit softer than the merged sample, is continued.

Turning from the event shape observables to jet observables, the small differences between the two samples vanish nearly completely. In Fig. 14, the relative fractions of events with different numbers of jets are exhibited in dependence on the jet resolution parameter y . The mutual agreement of the two samples and their agreement with data is excellent: The parton shower is perfectly capable of describing jet multiplicities at LEP 1. This finding is repeated for the differential jet rates, viz Fig. 15. In Fig. 16, the topological structure of four jet events is investigated. To this end, the Bengtsson-Zerwas angle [61] and the modified Nachtmann-Reiter angle [62] are studied. Apparently, the merged sample is in perfect agreement with the data, whereas the “parton shower only” sample exhibits a slight shift away from them. This, however, is not a big surprise; after all, these observables do depend on interferences between different diagrams. To take this into account clearly is well beyond the abilities of the parton shower.

¹⁰For definitions, the reader is referred to appendix C.

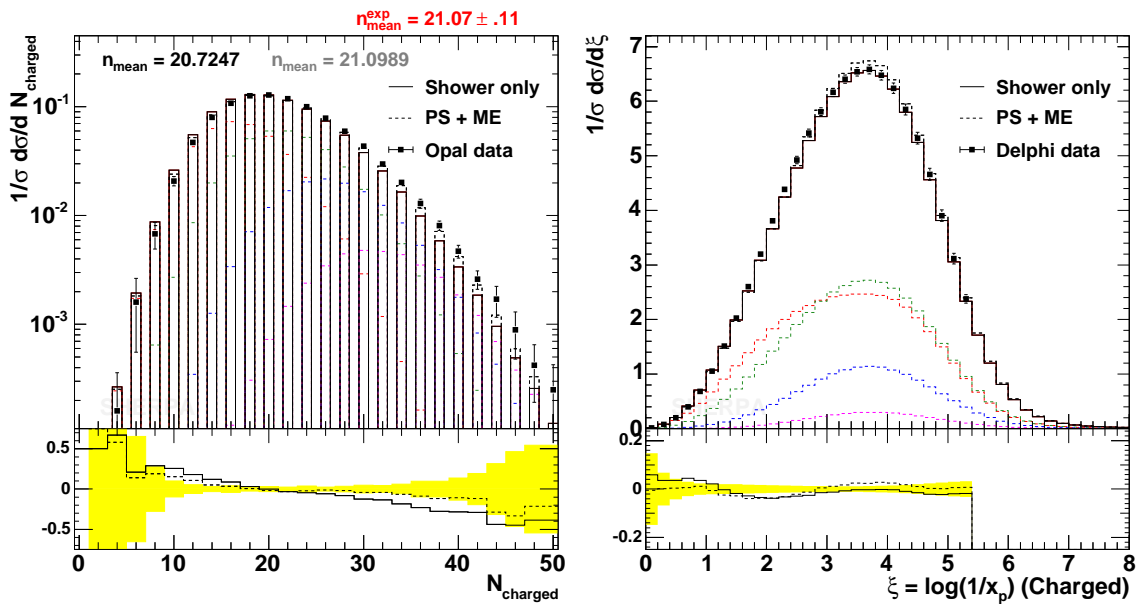


Figure 11: Charged multiplicity and scaled momentum at LEP 1. The left plot shows the distribution of the number of charged particles together with a measurement by Opal [58]. The mean charge multiplicity is also stated together with its PDG value [59]. On the right hand side, a scaled momentum distribution is plotted against Delphi data [54]. The data are contrasted with results obtained through the parton shower alone (solid lines) with those obtained when the merging of matrix elements for up to five jets and the parton shower has been employed (dashed lines). In the latter case coloured lines indicate the contributions from individual matrix elements.

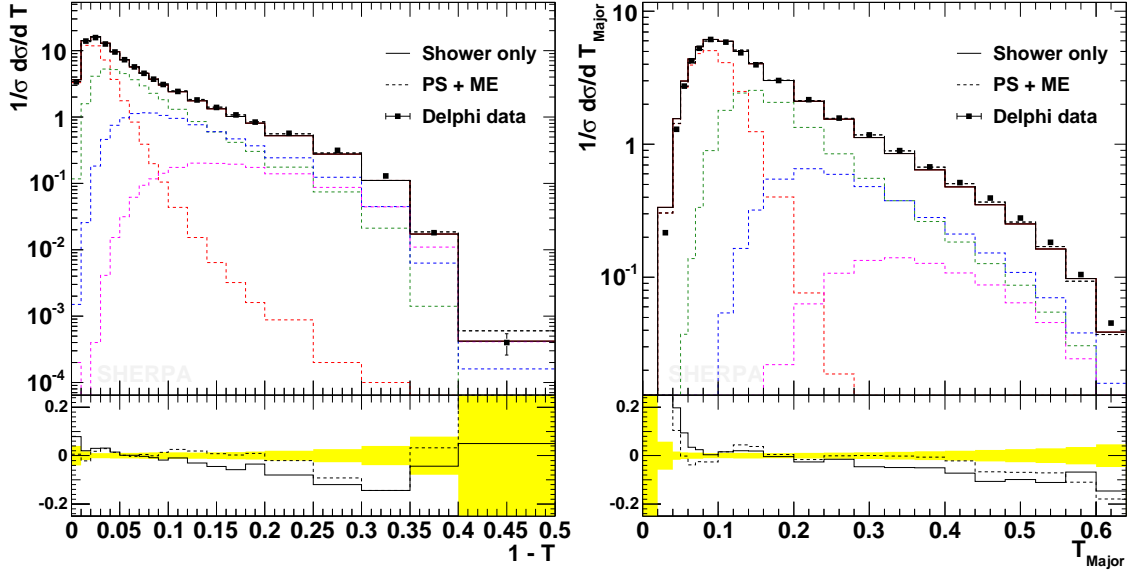


Figure 12: Thrust and Major at LEP 1. The hadron level result of SHERPA is contrasted with measurement from the Delphi collaboration [54]. Line styles and colours are the same as in Fig. 11.

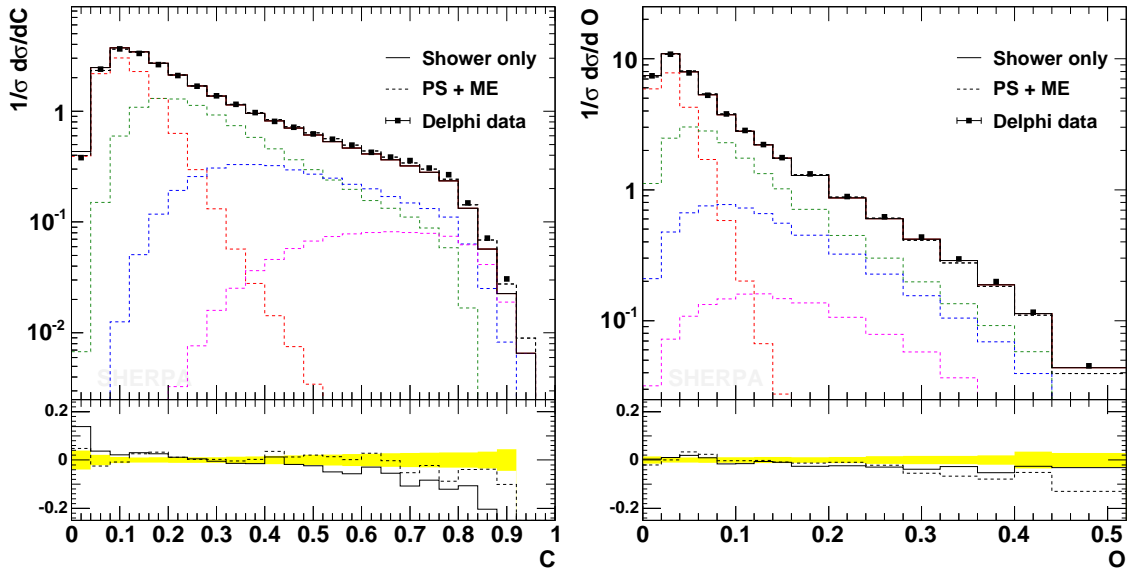


Figure 13: C-Parameter and Oblateness at LEP 1. This plot shows the event shape variables C-parameter and oblateness, together with Delphi data[54]. Line styles and colours are the same as in Fig. 11.

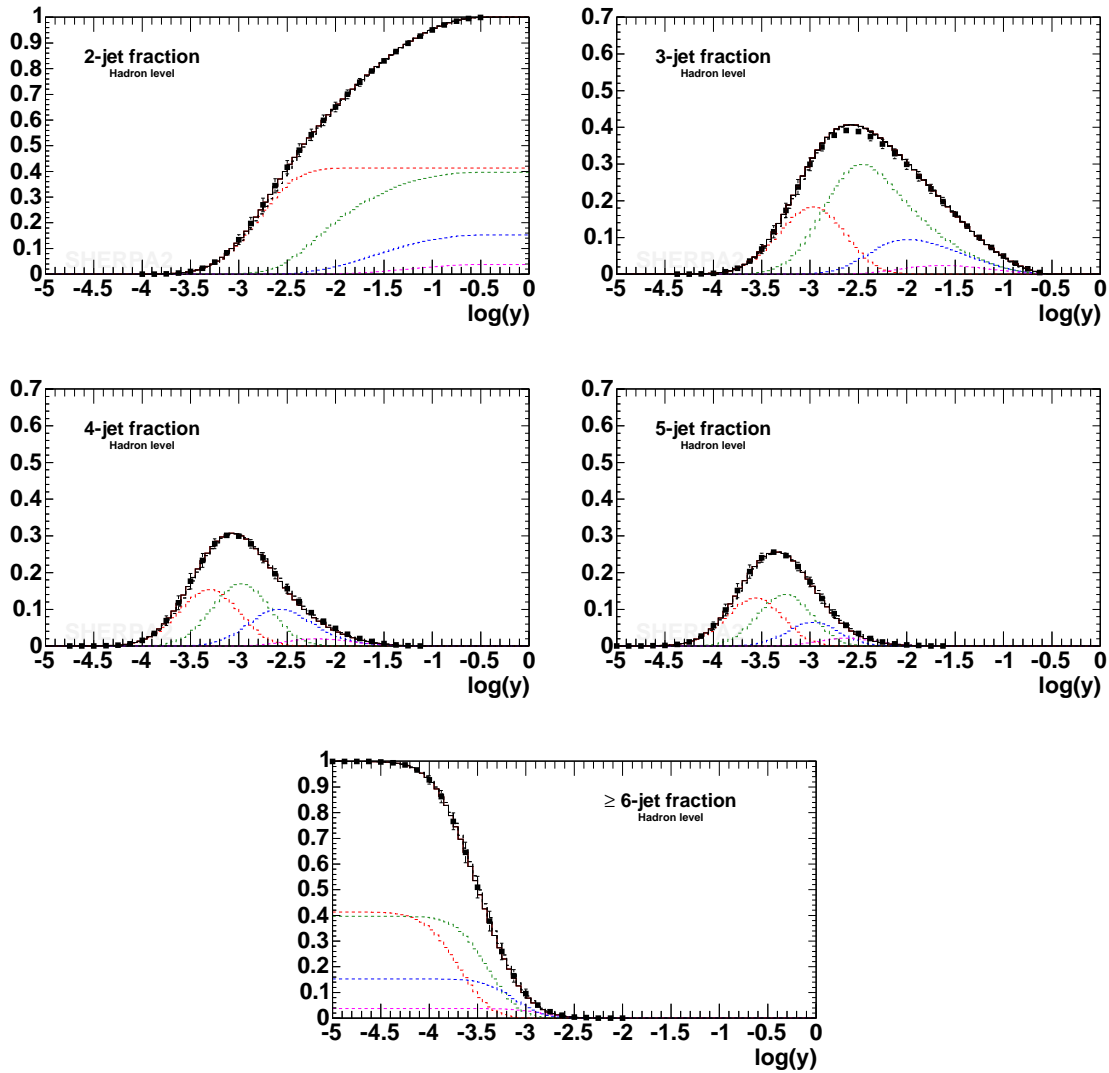


Figure 14: Durham jet rates at LEP 1, taken from [60]. Line styles and colours are the same as in Fig. 11.

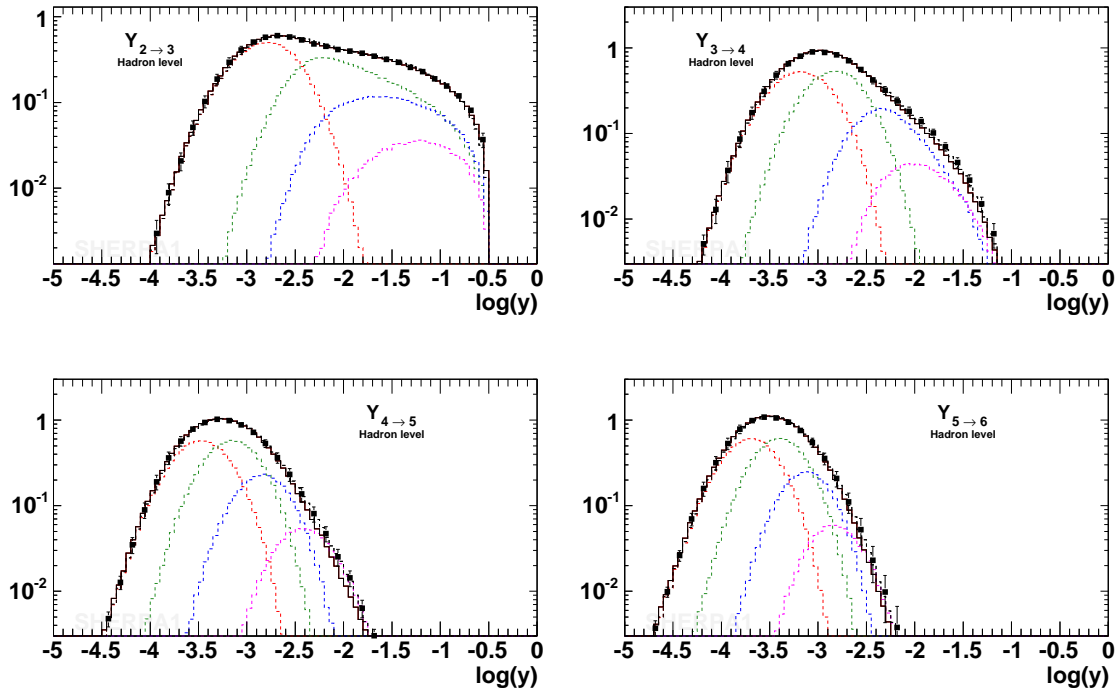


Figure 15: Differential jet rates in the Durham scheme at LEP 1, taken from [60]. Line styles and colours are the same as in Fig. 11.

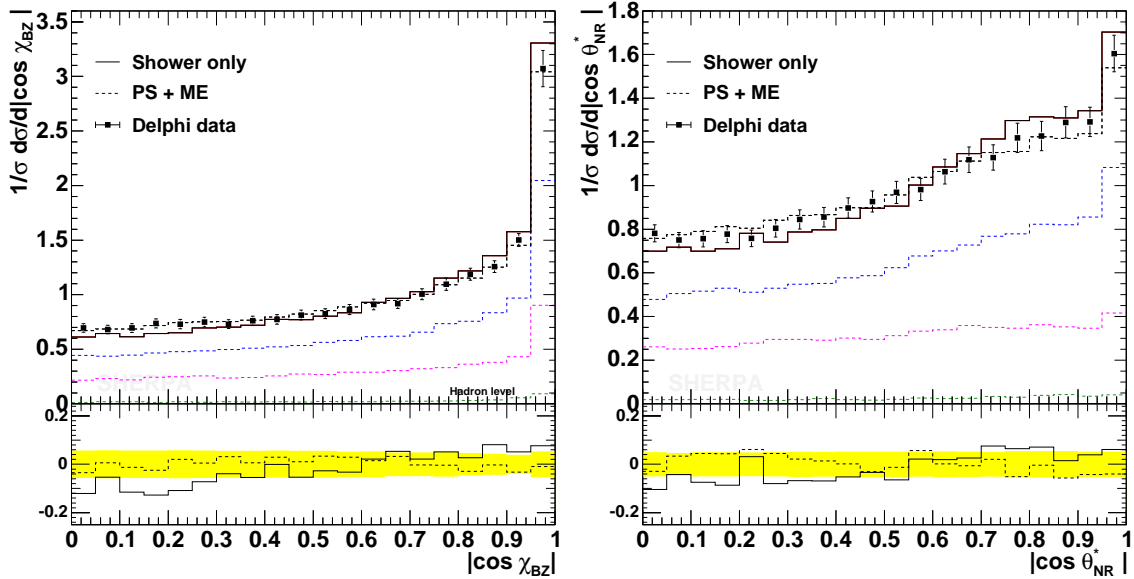


Figure 16: Four jet angle distributions. Shown are the Bengtsson-Zerwas angle (left) and the modified Nachtmann-Reiter angle (right). The data points are from a DELPHI measurement [57].

Tevatron

Having investigated the final state parton shower, the focus shifts now on a study of the parton shower in the initial state. There, a good observable to judge the performance of the parton shower is the transverse momentum distribution of lepton pairs in Drell-Yan scattering. In Fig. 17 the p_{\perp} distribution of such pairs with masses at the Z -pole (91 ± 15 GeV) is displayed. In order to describe the left side of the distribution, the initial partons have to be supplemented with intrinsic transverse momentum w.r.t. the hadron they stem from. In SHERPA, this intrinsic k_{\perp} is distributed according to a Gaussian, with expectation value $k_{\perp} = 0.8$ GeV. In this plot, two different simulation runs are confronted with data, both only use the parton shower for parton radiation. They differ in the choice of the starting scale of the shower evolution; one is starting at $t = M_{ll}^2 \approx M_Z^2$, the other one is starting at the c.m. energy squared of the incoming hadrons. Clearly, this leads to differences in the treatment of hard radiation, and as expected in the former case, parton radiation ceases to exist at scales of the order of the hard scale. The agreement of both simulation runs with data at scales up to 40-50 GeV, however, is excellent. In Fig. 18, the same observable is depicted once more, this time, however, the data are confronted with the pure parton shower, starting at the high scale, and with the merged result, including up matrix elements for the production of the Z accompanied with up to three hard jets. The results again are in great agreement with data. This shows that also the implementation of the initial state parton shower in APACIC++ has succeeded.

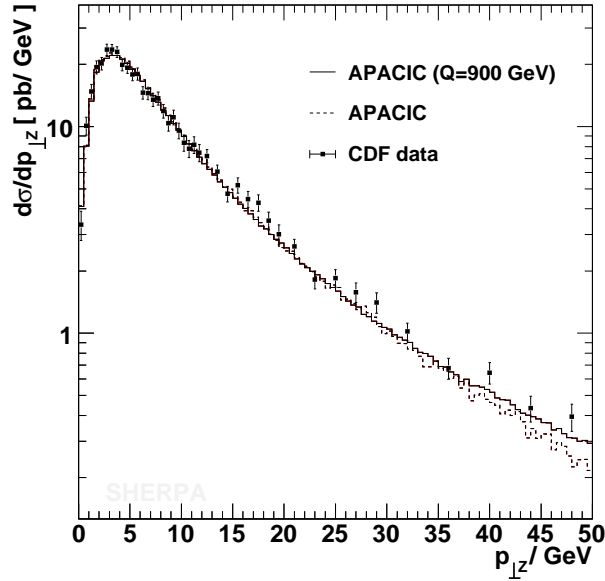
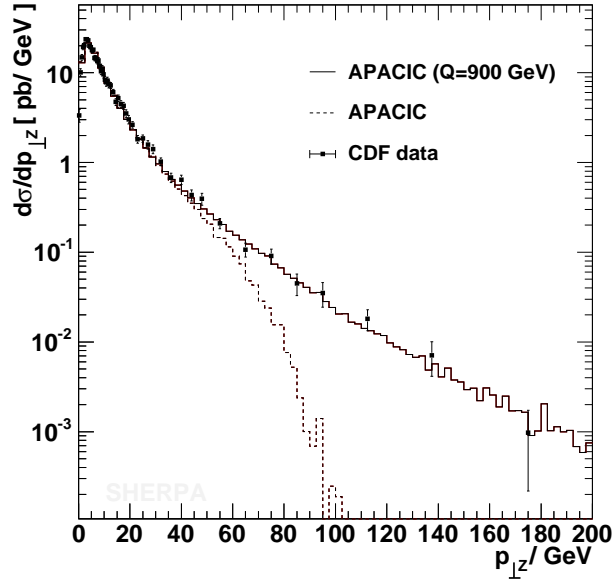


Figure 17: The p_{\perp} distribution of the Z -boson in comparison with data from CDF at the Tevatron, Run I [63]. The bottom plot shows the same distribution as the top one, but with focus on the low momentum region. The solid line indicates the shower result when using a fixed start scale of 1800 GeV, while the the dashed line is obtained when using $s' \approx M_Z^2$ as start scale. The SHERPA results have been multiplied by a constant K -factor of 1.45 to match the data.

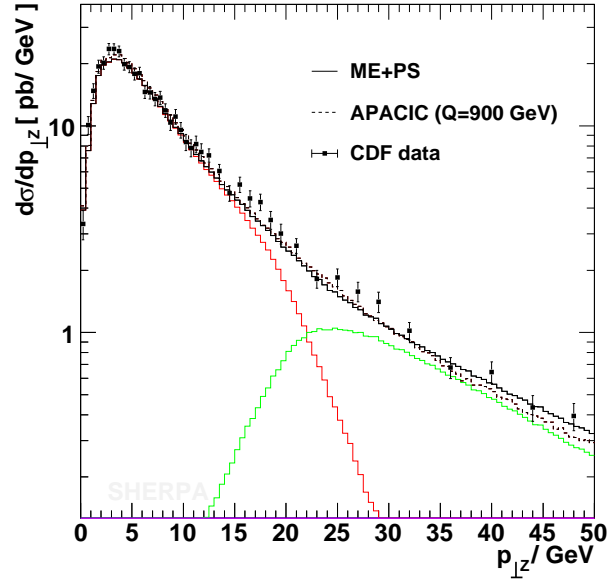
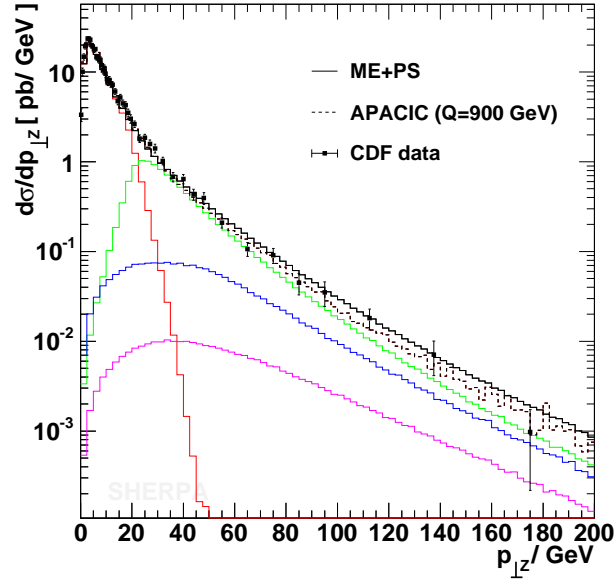


Figure 18: The p_{\perp} distribution of the Z -boson in comparison with data from CDF at the Tevatron, Run I [63]. This plot shows the same distributions as Fig. 17, but this time the pure shower performance is compared with the result obtained when merging matrix elements with up to 3 extra jets. The jet scale Q_{cut} was fixed to 20 GeV. The coloured lines give the contributions from individual matrix elements.

5 Conclusions

In this paper, the new version of the program **APACIC++** has been presented. In contrast to its first version, **APACIC++** ceased to be a stand-alone program; now, it is just the parton shower module of a larger framework. This transformation resulted in a relocation of many steering and service classes. On the other hand, the scope of **APACIC++** widened in such a way that in its present state it is also capable of performing the parton shower in the initial state of hadronic collisions. In addition, the merging procedure with the matrix elements has been refined. On the technical side, some algorithms have been changed, in particular, the look-up tables for the Sudakov form factors have been replaced by an algorithm based on the hit-or-miss method.

Some exemplary results obtained with the new version of **APACIC++** have been presented as well. The comparison with known analytical results, that properly resum large logarithms, validates the physical and numerical correctness of the implementation of the Sudakov form factors. This is not too obvious, since the analytical results contains logarithms in terms of transverse momentum scales, whereas the parton shower in **APACIC++** has been formulated in terms of virtual mass, supplemented with appropriate scale choices and an explicit angular ordering. Both the parton shower alone and it being merged with matrix elements results in an excellent agreement with a collection of precise data. These results span up to five orders of magnitude and the agreement is, especially for the LEP 1 data, on the level of a few percent. This proves the validity and underlines the abilities of the parton shower implemented in **APACIC++**.

Acknowledgements

F.K. and A.S. mourn the dead of Gerhard Soff, teacher and friend.

F.K. and A.S. are indebted to S. Höche, T. Gleisberg, S. Schumann and J. Winter for fruitful collaboration on **SHERPA** and in particular for many patient tests of **APACIC++**.

A.S. and F.K. thank K. Hamacher and H. Hoeth for many helpful discussions and for the patient tuning of the parton shower. F.K. would like to thank S. Catani, S. Gieseke, M. Mangano, P. Richardson, and B. Webber for pleasant discussions concerning parton showers and their merging with matrix elements. The authors acknowledge financial support by BMBF, GSI and DFG.

A Brief program documentation

APACIC++ is the module responsible for parton showers inside the SHERPA framework. Therefore, basic physics tools, like e.g. four-momentum, PDFs, particle definitions, and the jet algorithm, are provided through the overall framework. Furthermore, a number of features related to the jet-veto are closely connected to the implementation of the merging procedure in SHERPA. Nevertheless, APACIC++ could be employed by the framework of a different event generator, provided the basic physics tools are made available.

This section gives a brief summary of the tasks each class in APACIC++ is responsible for. Where needed, some details on specific implementation issues are presented that should, in principle, enable the interested user to implement and test some of his or her own ideas. As stated above, in Sec. 3, APACIC++ represents the evolving parton shower in terms of binary Trees, consisting of doubly linked Knots. Each of them represents one individual parton splitting. APACIC++ steers the shower evolution in the initial and final through two different classes, `Initial_State_Shower` and `Final_State_Shower`, respectively. These shower classes fill the Knots through corresponding Sudakov form factors, encoded in `Timelike_Sudakov` and `Spacelike_Sudakov`, where the latter carries a link to the appropriate PDF. Therefore, there are two instances of `Spacelike_Sudakov` with potentially different PDF in the `Initial_State_Shower`. For convenience, both Sudakov classes are derived from the class `Splitting_Group`; as such, they contain all relevant `Splitting_Functions`. However, both showers reconstruct the branching kinematics of each splitting from quantities like the scale t and the energy splitting parameter z . This is achieved in the two classes `Timelike_Kinematics` and `Spacelike_Kinematics`, respectively.

The interface with SHERPA: the class `Apacic`

This class defines the general interface to the shower package APACIC++. The parton shower evolution for a set of given partons is performed along the following steps:

- The parton shower of each event is started after setting appropriate initial conditions, taken from the merging with the matrix element. These initial conditions - basically starting scales t and maximal angles for the coherent shower evolution - are brought directly into the Trees by filling the pseudo parton shower history of the matrix elements into corresponding Knots. Pointers to the Trees needed for this operation are extracted from the showers and handed to the outside world through the methods `FinTree()` and `IniTrees()`.
- By calling `PerformShowers()`, the corresponding methods in the class `Final_State_Shower` and in the class `Initial_State_Shower` are triggered to perform the shower evolution. All necessary boosts at the beginning and at the end of the

shower¹¹ are carried out in here. The methods `SetJetvetoPt2()` and `SetFactorisationScale()` are used to pass settings relevant for the parton shower piece of the merging into the showers. The check of whether a jet was lost during shower evolution is performed through `Final_State_Shower::ExtraJetCheck()`.

- The final result of the shower evolution can be transferred to the SHERPA framework with the help of `ExtractPartons()`.

Running the showers

The class `Final_State_Shower`

This is the central class of the final state shower implementation. It controls the sequence of evolution steps¹². For the individual shower evolution of a single parton the class `Timelike_Sudakov` is employed. Branching kinematics are constructed after the evolution has finished, using the class `Timelike_Kinematics`. It is also responsible for some kinematics checks during the shower evolution and for the jet veto.

The final state shower evolution of a given jet ensemble is performed by `PerformShower()`, while the method `FirstTimelikeFromSpacelike()` is called for the final state (time-like) shower of a parton emitted during the initial state (space-like) shower evolution. The different methods of the class `Final_State_Shower` are responsible for the following tasks:

- The method `PerformShower()` initiates the final state shower on a given tree, i.e. starting from its root `Knot`. This is done in `InitializeJets()`, the kinematics are constructed afterwards utilising `TimelikeKinematics::DoKinematics()`.
- `InitializeJets()` initialises the jet system emerging from a given (dummy) mother knot. The algorithm is performed recursively along the following steps:
 1. If one or both of the two daughters are allowed to decay, the mother `Knot` is filled accordingly and the parton system produced by the decaying daughter(s) must be further evolved. These tasks are achieved by `FillBranch()` and `EvolveJet()`, respectively.
 2. If any the two daughters can not decay (internal lines of a ME), `InitializeJets()` is called again, with the daughter in question taking the role of the mother knot.
- To fill a branch, its splitting scale t and energy splitting variable z have to be determined. In APACIC++, this is realised through `FillBranch()`. There, a mother with parameters $\{t_a, z_a\}$ for a decay $a \rightarrow bc$ into two already specified massless daughters serves as input for the determination of their $\{t_i, z_i\}$ ($i = b, c$).

¹¹For instance, the final state shower is always performed in the rest frame of the particles starting it.

¹²Note that the class `Final_State_Shower` is also utilised for the (time-like) evolution of any parton emitted off the initial state shower.

Step by step one of the daughters is chosen to obtain a new trial virtuality \bar{t}_i according to Eq. (2), realised by `Timelike_Sudakov::Dice()`. In each step, the last \bar{t}_i serves as starting condition for the determination of the new one. Only if the system of both daughters passes the kinematic constraints, this sequence of alternating reduction of the \bar{t}_i is interrupted and they are accepted. Then, the mothers energy splitting variable z_a must be modified according to Eqs. (15, 32) implemented in `Timelike_Kinematics::Shuffle()` to compensate for the gain in virtuality of the daughters.

- `EvolveJet()` evolves a given parton system, consisting of a mother knot with two daughters. The algorithm works recursively: Both daughters may branch further, therefore `FillBranch()` is called first to determine both virtualities within the given kinematical constraints. In case neither of the daughters branches, the algorithm stops at once. Otherwise, `EvolveJet()` is called for the corresponding daughter(s).
- `FirstTimelikeFromSpacelike()` in contrast tries to initialise a new jet system emerging from a time-like particle emitted by a space-like shower. If, starting from the virtuality t_a of the space-like branch $b \rightarrow ac$, the `Timelike_Sudakov::Dice()` yields a suitable virtuality $t_c > t_0$ respecting the constraint Eq. (23), daughters are initialised and the jet is evolved by `EvolveJet()`.
- After the shower is completed, colours are set through the method `SetAllColours()` according to the algorithm described above. Then, the method `ExtractPartons()` extracts the partons (instances of the class `Particle` of the full framework) from the outgoing `Knots` of the `Tree` and fills them into the event record.

The class `Initial_State_Shower`

The class `Initial_State_Shower` governs the space-like shower evolution. Starting with the particles entering the hard $2 \rightarrow 2$ piece of the process, a backward shower is performed with the help of the classes `Spacelike_Sudakov` (two objects, one for each beam) and `Spacelike_Kinematics`. For the treatment of time-like parton emissions the control is transferred to the class `Final_State_Shower`. The `Initial_State_Shower` object contains the following methods:

- `PerformShower()` is called in order to start the space-like shower evolution. Information on the matrix element kinematics is given in form of two partially filled trees, corresponding to the evolution of the left and the right incoming parton, respectively. Similar to the final state case, the shower is initiated by employing `InitializeSystem()`. After the evolution has finished some consistency checks are done, and the shower history is transferred back into the laboratory frame.
- `InitializeSystem()` determines the initial system for the shower evolution. The algorithm starts with calling `FillBranch()` for each of the given matrix element

partons in order to obtain the virtuality t_i and energy fraction z_i of the first splittings. Then, the off-shell momenta are constructed with the help of `Spacelike_Kinematics::InitKinematics()`.

- Additional branchings are appended by `EvolveSystem()`. This method performs the evolution of a given system of two space-like partons, by recursively appending additional branchings. In each step a system consisting two partons of different incoming beams. The shower evolution is performed backward, i.e. from the hard interaction towards the beam particle. The parton with larger virtuality is supposed to be closer to the hard interaction and is selected for the next evolution step. There, the virtuality t and energy fraction z is fixed by consecutive calls of `FillBranch()`, `CalculateMaxT()`, and `FirstTimelikeFromSpacelike()`. After each step, the four-momenta of the participating partons are evaluated with `DoKinematics()`, leading to a new system of two space-like partons.
- After the shower evolution is finished, the created parton set can be accessed by calling `ExtractPartons()`. It fills all final state particles connected to the two incoming `Trees` into the event record.
- Two configuration methods need to be mentioned, which are of special importance in the context of merging ME and PS, namely `SetJetvetoPt2()` and `SetFactorisationScale()`. In order to guarantee a clean separation between, the jet-veto is imposed on any trial emission inside the shower. Usually, the p_\perp for any trial radiation is restricted by the jet resolution scale p_\perp^{cut} . For the matrix element with the highest multiplicity of jets, the separation cut is dynamically fixed by the smallest transverse momentum present in the hard interaction, owing to the fact that shower is not supposed to produce radiation harder than any QCD radiation present in the matrix element. In full analogy, merging ME and PS involves evaluating the PDFs at a specific factorisation scale μ_F . The dependence on the μ_F is to be cancelled by a corresponding PDF evaluation during the first parton emission in the initial state shower. The factorisation scale μ_F does not necessary coincide with the jet-veto scale mentioned above p_\perp^{cut} . For instance for (leptonically decaying) W bosons produced in hadronic collisions, there is no jet-veto applied, but of course μ_F is not vanishing. In fact, in this example case, the factorisation scale is identified with the hard c.m energy $\sqrt{s'}$.

Splitting functions & Sudakov form factors

The class `Splitting_Function` is purely virtual. It defines a common interface to the splitting functions $P_{a \rightarrow bc}(z)$. Among others, this class and its specific instantiations include methods to

- access its flavours (`GetFlA()`, `GetFlB()`, and `GetFlC()`)
- to determine z according to an approximative distribution (`GetZ()`), and its integral in a given region (`CrudeInt()`),

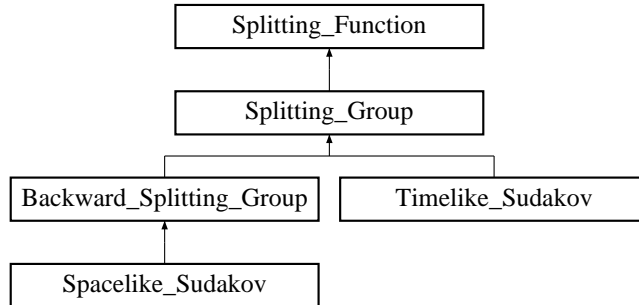


Figure 19: class hierarchy

- a correction weight (`GetWeight()`), and the exact functional form of the splitting function through its `operator()`
- and some methods to manage `Splitting_Groups`.

All implemented splitting functions are derived from this class, cf. Tab. 20. This abstraction renders the inclusion of further splitting functions an easy task.

The class `Splitting_Group` is a container derived from the abstract class `Splitting_Function`. It contains all splitting functions of a given flavour, either in the forward splitting or for backward splitting as a `Backward_Splitting_Group` object. It is thus responsible for the determination of a branching for one specific flavour. The integration routine therefore returns the sum of the integrals of all single `Splitting_Functions`. After the integration the routine `SelectOne()` can be called to choose one splitting mode out of the available options according to the integrals. All subsequent calls to flavour access methods, dice routines or the weight calculation then correspond to the selected branching. Note that the `Splitting_Group` is also the base of any Sudakov form factor determination, as depicted in Fig. 19.

Both Sudakov classes are derived from the corresponding `Splitting_Group`. Of course, in the space-like case, the mother class is the `Backward_Splitting_Group`. Following their names, the classes `Timelike_Sudakov` and `Spacelike_Sudakov` govern the time-like and space-like shower evolution, respectively. The latter one must be supplemented with a link to a PDF implementation, realised in `SHERPA` through an object derived from an abstract `PDF_Base`. However, both Sudakov classes store appropriate `Splitting_Groups` for every flavour taking part in the shower. In both classes, the method `Dice()` is responsible for the determination of virtualities (`ProduceT()`), daughter flavours, and energy fractions. The algorithm chosen is the hit-or-miss method, and both classes thus contain various veto methods implementing cuts and correction weights. To exemplify this, both classes have a method `Cp1Veto()` incorporating the correction weight $\alpha_s(Q)/\alpha_s(Q_{\min})$. Especially for the incorporation of issues related with coupling constants, both have a link to the class `Sudakov_Tools`.

QED splitting functions	
Fermion_To_Fermion_Photon	$P_{f \rightarrow f\gamma}(z)$ cf. Eq. (33)
Photon_Fermion_Fermion	$P_{\gamma \rightarrow f\bar{f}}(z)$ cf. Eq. (34)
QCD splitting functions	
Quark_To_Quark_Gluon	$P_{q \rightarrow qg}(z)$ cf. Eq. (35)
Gluon_To_Quark_Quark	$P_{g \rightarrow q\bar{q}}(z)$ cf. Eq. (36)
Gluon_To_Gluon_Gluon	$P_{g \rightarrow gg}(z)$ cf. Eq. (37)
SUSY QCD splitting functions	
Gluino_To_Gluino_Gluon	$P_{\tilde{g} \rightarrow \tilde{g}g}(z)$ cf. Eq. (41)
Gluon_To_Gluino_Gluino	$P_{g \rightarrow \tilde{g}\tilde{g}}(z)$ cf. Eq. (42)
SQuark_To_SQuark_Gluon	$P_{\tilde{q} \rightarrow \tilde{q}g}(z)$ cf. Eq. (43)
Gluon_To_SQuark_SQuark	$P_{g \rightarrow \tilde{q}\tilde{q}}(z)$ cf. Eq. (44)

Figure 20: A summary of implemented splitting functions and their class names in SHERPA.

Kinematics

Kinematics are implemented in two classes, `Timelike_Kinematics` and `Spacelike_Kinematics` for the determination of the kinematics in the final and initial state showers, respectively. They include

- checks whether a branching is kinematically possible (`KinCheck()`),
- a check whether an emission yields a jet that must be vetoed in the merging procedure (`JetVeto()`), and
- a method to construct kinematics (`DoKinematics()`).

In addition, `Timelike_Kinematics` provides a method to redefine the energy splitting z according to Eqs. (15, 32) (`Shuffle()`), and `Spacelike_Kinematics` has a method to determine the maximal kinematically allowed t for the initialisation of a final state shower off an initial state splitting (`CalculateMaxT()`), cf. Eq. (23)

Basic structures

`Trees` are used as representations of parton shower histories in terms of interconnected binary splittings. It provides the basic structure and all necessary routines to handle operations, like boosts, on the whole or parts of a tree. Three trees form a complete parton shower history: Two trees correspond to the initial state shower evolution of the right and the left incoming particle, respectively, and the other tree holds information of the final state shower of the outgoing particles, cf. Sec. 3.

The `Knots` are the basic elements forming a binary `Tree`. They store all properties of a single branching, like flavour, momentum, virtuality, energy component, etc..

B Altarelli–Parisi splitting functions

In this appendix all splitting functions, relevant for the shower evolution of APACIC++ are listed, cf. [64, 65]. The splitting functions are obtained after averaging over the azimuthal angle. The mass terms in each case are parametrised by the variable $\mu_{ij}^2 = (m_i^2 + m_j^2)/[(p_i + p_j)^2 - m_{(ij)}^2]$. The expressions for splittings with the decay products exchanged fulfil the obvious symmetry relation $P_{a \rightarrow bc}(z) = P_{a \rightarrow cb}(1 - z)$.

Fermions and photons:

$$P_{f \rightarrow f\gamma}(z; \mu_{f\gamma}^2) = e_f^2 \left[\frac{1+z^2}{1-z} - 2\mu_{f\gamma}^2 \right], \quad (33)$$

$$P_{\gamma \rightarrow f\bar{f}}(z; \mu_{f\bar{f}}^2) = e_f^2 \left[z^2 + (1-z)^2 + \mu_{f\bar{f}}^2 \right]. \quad (34)$$

Quarks and gluons:

$$P_{q \rightarrow qq}(z; \mu_{qq}^2) = C_F \left[\frac{1+z^2}{1-z} - 2\mu_{qq}^2 \right], \quad (35)$$

$$P_{g \rightarrow q\bar{q}}(z; \mu_{q\bar{q}}^2) = T_R \left[z^2 + (1-z)^2 - \mu_{q\bar{q}}^2 \right], \quad (36)$$

$$P_{g \rightarrow gg}(z) = C_A \left[\frac{z}{1-z} + \frac{1-z}{z} + z(1-z) \right]. \quad (37)$$

In the massless limit ($\mu \rightarrow 0$), these splitting functions reduce to the well-known form

$$P_{qq}(z) = C_F \frac{1+z^2}{1-z}, \quad (38)$$

$$P_{gq}(z) = T_R \left[z^2 + (1-z)^2 \right], \quad (39)$$

$$P_{gg}(z) = C_A \left[\frac{z}{1-z} + \frac{1-z}{z} + z(1-z) \right]. \quad (40)$$

Gluinos and gluons:

$$P_{\tilde{g} \rightarrow \tilde{g}g}(z; \mu_{\tilde{g}g}^2) = C_A \left[\frac{1+z^2}{1-z} - 2\mu_{\tilde{g}g}^2 \right], \quad (41)$$

$$P_{g \rightarrow \tilde{g}\tilde{g}}(z; \mu_{\tilde{g}\tilde{g}}^2) = C_A \left[z^2 + (1-z)^2 + \mu_{\tilde{g}\tilde{g}}^2 \right]. \quad (42)$$

Squarks and gluons:

$$P_{\tilde{q} \rightarrow \tilde{q}g}(z; \mu_{\tilde{q}g}^2) = C_F \left[\frac{2z}{1-z} - 2\mu_{\tilde{q}g}^2 \right], \quad (43)$$

$$P_{g \rightarrow \tilde{q}\tilde{q}}(z; \mu_{\tilde{q}\tilde{q}}^2) = T_R \frac{1}{2} \left[2z(1-z) - \mu_{\tilde{q}\tilde{q}}^2 \right]. \quad (44)$$

C Definitions of event shapes

The global properties of hadronic events may be characterised by set of observables, usually called event shapes. In section 4 the following shape observables have been considered.

- Thrust T :

The thrust axis \vec{n}_T maximises the following quantity

$$T = \max_{\vec{n}_T} \left(\frac{\sum_i |\vec{p}_i \cdot \vec{n}_T|}{\sum_i |\vec{p}_i|} \right), \quad (45)$$

where the sum extends over all particles in the event. The thrust T tends to 1 for events that has two thin back-to-back jets (“pencil-like” event), and it tends towards 1/2 for perfectly isotropic events.

- Thrust Major T_{Major} :

The thrust major vector \vec{n}_{Major} is defined in the same way as the thrust vector, but with the additional condition that \vec{n}_{Major} must lie in the plane perpendicular to \vec{n}_T :

$$T_{\text{Major}} = \max_{\vec{n}_{\text{Major}} \perp \vec{n}_T} \left(\frac{\sum_i |\vec{p}_i \cdot \vec{n}_{\text{Major}}|}{\sum_i |\vec{p}_i|} \right). \quad (46)$$

- Thrust Minor T_{Minor} :

The minor axis is perpendicular to both the thrust axis and the major axis, $\vec{n}_{\text{Minor}} = \vec{n}_T \times \vec{n}_{\text{Major}}$. The value of thrust minor is then given by

$$T_{\text{Minor}} = \frac{\sum_i |\vec{p}_i \cdot \vec{n}_{\text{Minor}}|}{\sum_i |\vec{p}_i|}. \quad (47)$$

- Oblateness O :

The oblateness is defined as the difference between thrust major T_{Major} and thrust minor T_{Minor} :

$$O = T_{\text{Major}} - T_{\text{Minor}} \quad (48)$$

- C-parameter C :

The C-parameter is derived from the eigenvalues of the linearised momentum tensor $\Theta^{\alpha\beta}$, defined by

$$\Theta^{\alpha\beta} = \frac{1}{\sum_i |\vec{p}_i|} \sum_i \frac{p_i^\alpha p_i^\beta}{|\vec{p}_i|}, \quad \alpha, \beta = \{x, y, z\}. \quad (49)$$

The three eigenvalues λ_i of this tensor define C with

$$C = 3(\lambda_1\lambda_2 + \lambda_2\lambda_3 + \lambda_1\lambda_3). \quad (50)$$

References

- [1] T. Sjöstrand, *Comput. Phys. Commun.* **82** (1994) 74;
- [2] T. Sjöstrand, L. Lönnblad and S. Mrenna, arXiv:hep-ph/0108264.
- [3] G. Corcella *et al.*, *JHEP* **0101** (2001) 010 [arXiv:hep-ph/0011363].
- [4] G. Corcella *et al.*, arXiv:hep-ph/0210213.
- [5] S. Frixione and B. R. Webber, arXiv:hep-ph/0207182.
- [6] S. Frixione and B. R. Webber, arXiv:hep-ph/0402116.
- [7] T. Gleisberg, S. Höche, F. Krauss, A. Schälicke, S. Schumann and J. C. Winter, *JHEP* **0402** (2004) 056 [arXiv:hep-ph/0311263].
- [8] S. Catani, F. Krauss, R. Kuhn and B. R. Webber, *JHEP* **0111** (2001) 063 [arXiv:hep-ph/0109231].
- [9] F. Krauss, *JHEP* **0208** (2002) 015 [arXiv:hep-ph/0205283].
- [10] F. Krauss, A. Schälicke, S. Schumann and G. Soff, *Phys. Rev. D* **70** (2004) 114009 [arXiv:hep-ph/0409106].
- [11] L. Lönnblad, *Comput. Phys. Commun.* **71**, 15 (1992).
- [12] L. Lönnblad, *Acta Phys. Polon. B* **33**, 3171 (2002).
- [13] S. Mrenna and P. Richardson, *JHEP* **0405** (2004) 040 [arXiv:hep-ph/0312274].
- [14] M. L. Mangano, M. Moretti and R. Pittau, *Nucl. Phys. B* **632** (2002) 343 [arXiv:hep-ph/0108069].
- [15] M. L. Mangano, M. Moretti, F. Piccinini, R. Pittau and A. D. Polosa, *JHEP* **0307** (2003) 001 [arXiv:hep-ph/0206293].
- [16] R. Kuhn, F. Krauss, B. Ivanyi and G. Soff, *Comput. Phys. Commun.* **134** (2001) 223 [arXiv:hep-ph/0004270].
- [17] F. Krauss, R. Kuhn and G. Soff, *JHEP* **0202** (2002) 044 [arXiv:hep-ph/0109036].
- [18] A. Schälicke, F. Krauss, R. Kuhn and G. Soff, *JHEP* **0212** (2002) 013 [arXiv:hep-ph/0203259].
- [19] T. Sjöstrand and P. Z. Skands, *Eur. Phys. J. C* **39** (2005) 129 [arXiv:hep-ph/0408302].
- [20] T. Sjöstrand, L. Lönnblad, S. Mrenna and P. Skands, arXiv:hep-ph/0308153.

- [21] S. Gieseke, P. Stephens and B. Webber, JHEP **0312** (2003) 045 [arXiv:hep-ph/0310083].
- [22] S. Gieseke, A. Ribon, M. H. Seymour, P. Stephens and B. Webber, JHEP **0402** (2004) 005 [arXiv:hep-ph/0311208].
- [23] Y. L. Dokshitzer, Sov. Phys. JETP **46** (1977) 641 [Zh. Eksp. Teor. Fiz. **73** (1977) 1216].
- [24] V. N. Gribov and L. N. Lipatov, Yad. Fiz. **15** (1972) 781 [Sov. J. Nucl. Phys. **15** (1972) 438].
- [25] L. N. Lipatov, Sov. J. Nucl. Phys. **20** (1975) 94 [Yad. Fiz. **20** (1974) 181].
- [26] G. Altarelli and G. Parisi, Nucl. Phys. B **126** (1977) 298.
- [27] T. Sjöstrand, Phys. Lett. B **157** (1985) 321.
- [28] G. Marchesini and B. R. Webber, Nucl. Phys. B **310** (1988) 461.
- [29] S. Jadach, talk given at the HERA-LHC workshop, Oct. 2004, CERN, <http://home.cern.ch/jadach/public/cern-oct04.pdf>.
- [30] A. H. Mueller, Phys. Lett. B **104** (1981) 161.
- [31] B. I. Ermolaev and V. S. Fadin, JETP Lett. **33** (1981) 269 [Pisma Zh. Eksp. Teor. Fiz. **33** (1981) 285].
- [32] Y. L. Dokshitzer, V. S. Fadin and V. A. Khoze, Phys. Lett. B **115** (1982) 242.
- [33] G. Marchesini and B. R. Webber, Nucl. Phys. B **238** (1984) 1.
- [34] S. Catani, Y. L. Dokshitzer, M. Olsson, G. Turnock and B. R. Webber, Phys. Lett. B **269** (1991) 432.
- [35] X. Artru and G. Mennessier, Nucl. Phys. B **70** (1974) 93.
- [36] X. Artru, Phys. Rept. **97** (1983) 147.
- [37] M. G. Bowler, Z. Phys. C **11** (1981) 169.
- [38] B. Andersson, G. Gustafson and B. Soderberg, Z. Phys. C **20** (1983) 317.
- [39] T. Sjöstrand, Nucl. Phys. B **248** (1984) 469.
- [40] B. Andersson, Camb. Monogr. Part. Phys. Nucl. Phys. Cosmol. **7** (1997) 1.
- [41] Y. I. Azimov, Y. L. Dokshitzer, V. A. Khoze and S. I. Troian, Phys. Lett. B **165** (1985) 147.

- [42] T. D. Gottschalk, Nucl. Phys. B **214** (1983) 201.
- [43] B. R. Webber, Nucl. Phys. B **238** (1984) 492.
- [44] B. R. Webber, Ann. Rev. Nucl. Part. Sci. **36** (1986) 253.
- [45] J. C. Winter, F. Krauss and G. Soff, Eur. Phys. J. C **36** (2004) 381 [arXiv:hep-ph/0311085].
- [46] R. D. Field and R. P. Feynman, Nucl. Phys. B **136** (1978) 1.
- [47] D. Amati and G. Veneziano, Phys. Lett. B **83** (1979) 87.
- [48] F. Krauss, A. Schällicke, and G. Soff, in preparation.
- [49] S. Catani, Y. L. Dokshitzer and B. R. Webber, Phys. Lett. B **285** (1992) 291.
- [50] S. Catani, Y. L. Dokshitzer, M. H. Seymour and B. R. Webber, Nucl. Phys. B **406** (1993) 187.
- [51] F. Krauss and G. Rodrigo, Phys. Lett. B **576** (2003) 135 [arXiv:hep-ph/0303038].
- [52] P. Abreu *et al.* [DELPHI Collaboration], Phys. Lett. B **418** (1998) 430.
- [53] G. Rodrigo, A. Santamaria and M. S. Bilenky, Phys. Rev. Lett. **79** (1997) 193 [arXiv:hep-ph/9703358].
- [54] P. Abreu *et al.* [DELPHI Collaboration], Z. Phys. C **73** (1996) 11.
- [55] K. Hamacher and M. Weierstall, arXiv:hep-ex/9511011.
- [56] U. Flammeyer, PhD-thesis, Fachbereich Physik, Bergische Universität Wuppertal, 2001 [WUB-DIS 2001-4].
- [57] H. Hoeth, Diploma Thesis, Fachbereich Physik, Bergische Universität Wuppertal, 2003 [WUD 03-11].
- [58] P. D. Acton *et al.* [OPAL Collaboration], Z. Phys. C **53** (1992) 539.
- [59] S. Eidelman *et al.* [Particle Data Group Collaboration], Phys. Lett. B **592**, 1 (2004).
- [60] P. Pfeifenschneider *et al.* [JADE collaboration], Eur. Phys. J. C **17** (2000) 19 [arXiv:hep-ex/0001055].
- [61] M. Bengtsson and P. M. Zerwas, Phys. Lett. B **208** (1988) 306.
- [62] O. Nachtmann and A. Reiter, Z. Phys. C **16** (1982) 45.
- [63] T. Affolder *et al.* [CDF Collaboration], Phys. Rev. Lett. **84** (2000) 845 [arXiv:hep-ex/0001021].

- [64] S. Catani, S. Dittmaier and Z. Trocsanyi, Phys. Lett. B **500** (2001) 149 [arXiv:hep-ph/0011222].
- [65] W. Beenakker, R. Hopker, M. Spira and P. M. Zerwas, Nucl. Phys. B **492** (1997) 51 [arXiv:hep-ph/9610490].